

For Reference

NOT TO BE TAKEN FROM THIS ROOM

Ex LIBRIS
UNIVERSITATIS
ALBERTAENSIS



THE UNIVERSITY OF ALBERTA

A RECONNAISSANCE LEAD ISOTOPE STUDY OF BASE METAL
OCCURRENCES IN WEST-CENTRAL IRELAND

by



JOHN ANGUS GREIG

A THESIS

SUBMITTED TO THE FACULTY OF GRADUATE STUDIES AND RESEARCH
IN PARTIAL FULFILMENT OF THE REQUIREMENTS FOR THE DEGREE
OF MASTER OF SCIENCE

DEPARTMENT OF GEOLOGY

EDMONTON, ALBERTA
SPRING, 1972

UNIVERSITY OF ALBERTA
FACULTY OF GRADUATE STUDIES

The undersigned certify that they have read, and recommend to the Faculty of Graduate Studies and Research for acceptance, a thesis entitled "A Reconnaissance Lead Isotope Study of Base Metal Occurrences in West-Central Ireland", submitted by John Angus Greig in partial fulfilment of the requirements for the degree of Master of Science.

ABSTRACT

Lead isotope ratios were determined for 29 galena samples from 24 localities in west-central Eire. These include the Mogul, Tynagh and Gortdrum mines. All except 4 deposits are confined to Lower Carboniferous carbonate strata.

The recently revised geophysical constants $a_0 = 9.346$, $b_0 = 10.218$ and $c_0 = 28.96$ (Oversby, 1970) and age of the earth $t_0 = 4.578 \times 10^9$ years (Cooper et al., 1969) were used in calculating the best fit growth curves. The best fit growth curve on the plot of Pb^{207}/Pb^{204} vs. Pb^{206}/Pb^{204} has a μ ratio of 8.79, identical to the newly revised best fit growth curve of Cooper et al. (1969) for ordinary leads. The Irish leads may be interpreted as single stage or short period anomalous leads. According to a single stage interpretation, the lead was derived from a homogeneous system with respect to the ratios U:Th:Pb, which is characterized by the present ratios $\mu = 8.79$, $W = 36.4$ and $Th^{232}/U^{238} = 4.14$. Model ages span the range from 20 m.y. to 210 m.y. Geographically related deposits have about the same model ages. Recognition of a short period anomalous lead line and mathematical interpretation in terms of a short period two-

stage model would require considerably greater precision in the data.

An increasing body of evidence suggests that certain marine sediments may constitute a homogeneous source for so-called ordinary leads. Temperatures of desposition for the Mogul orebody range from 150 - 350°C and the average δS^{34} value for all sulphur species in solution centered about 0^o/oo (Greig et al., 1971). On the basis of the above temperature and sulphur isotope evidence alone, Lower Paleozoic shales, greywackes and volcanics are believed to be the most plausible sedimentary source for the Irish leads.

ACKNOWLEDGEMENTS

The author wishes to thank Dr. R. E. Folinsbee for his supervision of the thesis, for originally suggesting the project, and for his patience and guidance throughout; Dr. H. Baadsgaard for his direction in the analytical phases of the research; and Dr. G. L. Cumming for his direction in the interpretation of results.

The author also thanks Drs. Folinsbee, Baadsgaard, Cumming and Morton for their critical review of the manuscript.

TABLE OF CONTENTS

	Page
INTRODUCTION	1
 CHAPTER	
I. GEOLOGY	4
Geological Setting	4
Caledonian Orogenic Belt	7
Devonian Old Red Sandstone	8
Carboniferous	8
Armorican (Permo-Carboniferous)	
Structure	12
Post Carboniferous	13
Geology of the Base Metal	
Deposits	13
Consolidated Mogul Mine ..	13
Tynagh Mine	17
Gortdrum Mine	20
Riofinex Mine	20
Minor Base Metal Occurrence	21
 II. THEORY	 22
Introduction	22
Models for the Interpretation	
of Common Lead Isotope Ratios.	23
The Geophysical Constants a_o ,	
b_o , c_o and t_o	28
Anomalous Leads	30
Other Models	32
Mantle Depletion Models	32
Continuous Mixing Model	33
Sedimentary Source Model ...	33
Crustal Magmatic Source	36
Summary	37

Table of Contents, continued

CHAPTER	Page
III. METHODS, ERRORS AND RESULTS	38
Sample Preparation	38
Analytical Methods and Instrumentation	39
Accuracy of Results	40
Results	47
IV. INTERPRETATION AND CONCLUSIONS	48
Growth Curves	48
Errors	48
Interpretation Based on Lead Model	54
Single-Stage or Anomalous..	54
Source of Leads, Single- Stage Model	55
Model Age, Single-Stage Model	55
Summary of Model Lead Interpretation	59
Age of Mineralization and Source of Metals - Other Evidence ..	60
Age of Mineralization	60
Source of Metals	62
Validity of the Lead Model	65
Speculative Interpretation Based on Sedimentary Source Model .	67
BIBLIOGRAPHY	70
APPENDIX I - MINERALOGY, HOST ROCKS AND STRUCTURAL CONTROL OF MINOR BASE METAL OCCURRENCES	83
APPENDIX II - PREPARATION OF REAGENTS AND EXTRACTION PROCEDURES	87

TABLES

		Page
Table 2.1	Symbols and Constants Used in Age Determination	24
Table 3.1	Calibration of the 12 Inch Mass Spectrometer with NBS 982 and Broken Hill Leads (after Green, 1968)	44
Table 3.2	Corrected Lead Isotope Ratios ...	45
Table 4.1	Single-Stage Model Age in Yr. x 10 ⁶	57

FIGURES

	Page
Fig. 1.1 Geological setting showing mines and occurrences studied	5
Fig. 1.2 Carboniferous stratigraphy and ore horizons at Mogul, Tynagh, Gortdrum and Riofinex mines (from Snelgrove, 1966)	11
Fig. 1.3 Section 38,300 east International Mogul Mine	14
Fig. 1.4 (a) Plan and cross section of Tynagh deposit (from Derry, Clark and Gillatt, 1965)	18
(b) Plan of Gortdrum deposit (from Thompson, 1967)	18
Fig. 2.1 Pb^{207}/Pb^{204} - Pb^{206}/Pb^{204} and Pb^{208}/Pb^{204} - Pb^{206}/Pb^{204} plots showing the close fit of many ore leads to a single growth curve (from Kanasewich and Farquhar, 1965)	27
Fig. 4.1 Transparent overlay of Pb^{207}/Pb^{204} versus Pb^{206}/Pb^{204} plot showing distribution parallel to error lines of geographically related Irish leads	49

Figures, continued

	Page
Fig. 4.2 Plot of $\text{Pb}^{207}/\text{Pb}^{204}$ versus $\text{Pb}^{206}/\text{Pb}^{204}$	50
Fig. 4.3 Plot of $\text{Pb}^{208}/\text{Pb}^{204}$ versus $\text{Pb}^{206}/\text{Pb}^{204}$	51
Fig. 4.4 Plot of $\text{Pb}^{208}/\text{Pb}^{206}$ versus $\text{Pb}^{207}/\text{Pb}^{206}$	52
Fig. 4.5 $\text{Pb}^{207}/\text{Pb}^{204} - \text{Pb}^{206}/\text{Pb}^{204}$ plot showing position of Irish leads with respect to primary growth curve of Cooper ($U = 8.79$)	56

INTRODUCTION

As a result of intensive exploration activity in Eire throughout the 1960's four new base metal mines are in production and several have production pending. The four producing mines are the Consolidated Mogul lead-zinc-silver mine at Silvermines, the Northgate or Tynagh lead-zinc-copper-silver mine of Irish Base Metals Ltd. at Tynagh, the copper-silver-mercury mine at Gortdrum, all in west-central Eire, and the copper mine at Avoca in east-central Eire. One of the deposits pending production is the Tara deposit discovered early in 1971 30 miles northwest of Dublin. Tara is by far the largest and economically most important of the orebodies yet discovered in Eire. This modern revival of an ancient mining area now ranks this area as perhaps the most important base metal camp in Europe.

Research into many aspects of these newly discovered deposits at several universities in Eire, Great Britain and Canada has stirred considerable debate on their genesis. Individual orebodies are considered to be syngenetic by some, and epigenetic by others. The origin of the mineralization is equally controversial and is variously believed to be magmatic (derived from concealed Armorican plutons),

volcanogenic (related to Carboniferous volcanism) and sedimentary or metamorphic (derived from Lower Paleozoic or Upper Paleozoic sediments).

This thesis was undertaken with the general objective of providing some insight into the origin of the metals.

Two model interpretations are considered possible for the Irish leads; single-stage and short period anomalous. Since this thesis was first begun evidence has accumulated which suggests a sedimentary source for the so-called ordinary leads. For this reason the lead data is also considered in the light of a sedimentary source.

The area of study is confined to west-central Eire, and includes the Mogul, Tynagh, Gortdrum and Riofinex deposits. The sampling included these 4 deposits and 20 small sulphide occurrences.

The first lead isotope determinations on Irish galenas, 17 in number, were made by Moorbath (1959a) at Oxford University as part of a study which included many deposits throughout the British Isles. His work was followed-up by Pockley (1961) who made 63 determinations on Irish leads for a doctoral thesis (Oxford). Pockley's and Moorbath's results are published as part of a compre-

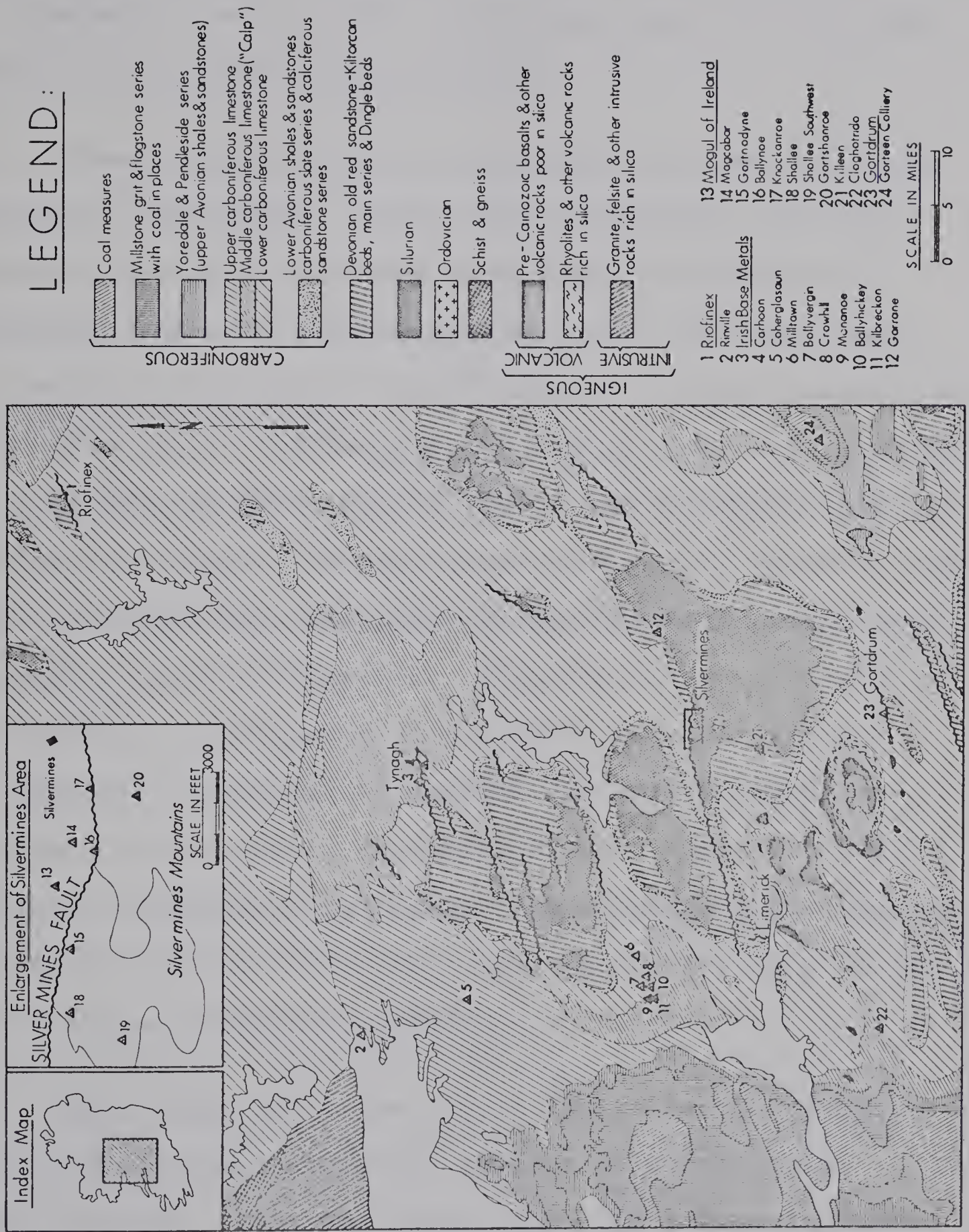
hensive lead isotope survey of base metal deposits in the British Isles, Eire and France (Moorbath, 1962). At the time of this earlier work, mass-spectrometric techniques were not as refined and interlaboratory comparisons revealed large discrepancies between various instruments.

CHAPTER 1

GEOLOGY

Geological Setting

Mogul, Tynagh, Gortdrum, Riofinex and Tara Mines and numerous minor base metal deposits occur in lower Carboniferous strata beneath the largely drift and bog covered Irish Central Plain. This plain, about 16,000 square miles in extent, is bounded on the north and northwest by mountainous Precambrian gneisses and schists, on the northeast and southeast by granites and low grade metasediments of the Caledonian orogenic belt and on the south by mountainous Paleozoics of the Armorican orogenic belt. Carboniferous carbonates rest conformably or with slight unconformity (northern regions) upon largely terrestrial Upper Devonian Old Red Sandstone, which in turn rests with pronounced unconformity upon intensely deformed Ordovician and Silurian rocks of the Caledonian (middle-Devonian) orogenic belt. Protruding through the central plain are mountainous inliers of Old Red Sandstone, sometimes with cores of Silurian and rarely, Ordovician rocks (Figure 1.1).



GEOLOGICAL SETTING SHOWING MINES AND OCCURRENCES STUDIED

Fig. 1.1

Ordovician and Silurian lithologies include shale, mudstone, siltstone, greywacke, and intercalated extrusives. The Caledonian grain is ENE to NE except where locally disrupted by Caledonian granite massifs.

Lower Carboniferous or Dinantian is subdivided into Tournaisian and Viséan. Basal shale, sandstone and shaly limestone pass upward through limestone and dolomite of Tournaisian age into a calcareous bryozoan-brachiopod mud bank complex (Waulsortian "reef" facies) of Upper Tournaisian - Lower Viséan age. The Waulsortian facies gives way northward to a lagoonal limestone facies (Calp) and southward to deeper water shales (Culm). Several large remnants of Namurian sandstone, shale and coal measures overlie Dinantian carbonates, for example, west of Limerick. Basaltic lavas and sills in the Dinantian are focussed at a number of small centres, most notably southeast of Limerick and tuff horizons are reportedly recognized in some mine areas. Tuffs are also reported in Devonian sandstones. Post Carboniferous igneous activity in Ireland is manifest only by the Tertiary flood basalts of the extreme northeast.

Open folds and a few thrust faults in the Carboniferous characterize Armorican compressive stresses in central Ireland. With few exceptions, the strata are flat lying to gently dipping north of the Armorican fold belt.

The dominating structural grain is ENE but changes to E approaching the Armorican front. Prominent, generally ENE striking normal faults throughout the Central Plain may have developed in response to a relaxation of Armorican compressive stresses, probably in late Carboniferous to early Permian times. The mountainous Devonian and Silurian inliers of the Central Plain may owe their existence to broad Armorican folding.

Caledonian Orogenic Belt

Devonian and younger strata rest with pronounced unconformity upon intensely deformed and slightly metamorphosed rocks of the Caledonian (Middle-Devonian) orogenic belt. The Caledonian grain is ENE to NE and is disrupted by several large Caledonian granite massifs of about 350 m.y. age. The Ordovician and Silurian were periods of almost continuous sedimentation. Shales, siltstones, greywackes, cherts and volcanics were deposited in a broad geosyncline oriented in a roughly NE direction. Within the area of study Silurian and rarely Ordovician rocks are exposed as inliers which protrude above the Carboniferous Central Plain. Extensive outcroppings of Ordovician and Silurian rocks occur peripheral to the Carboniferous Central Plain particularly in the northeast and southeast.

Devonian Old Red Sandstone

Pronounced relief on the basal unconformity is evidenced by a considerable variation in thickness of the Upper Devonian Old Red Sandstone. Piedmont accumulations at the base pass upward through dominantly fluviatile sandstones to lacustrine or lagoonal sandstones and marls at the top reflecting a progressive change from initially non-marine to marginal marine conditions. Numerous minor unconformities are believed to reflect minor Caledonian movements which extended into the Upper Devonian. Minor volcanic activity during Old Red Sandstone times is indicated by the presence of andesitic lavas and tuffs along the borders of the basin of deposition.

Carboniferous

In the south half of the Central Plain, Carboniferous strata rest conformably on Old Red Sandstone so that non-marine clastics in the north are chronostratigraphic equivalents of marine carbonates in the south.

The Irish Geological Survey distinguishes eight well defined lithological divisions in the Carboniferous which are in ascending order: Lower Limestone Shales, Lower Limestone, Middle Limestone (Calp), Upper Limestone, Yoredale Series, Pendleside Series, Millstone Grit and Coal Measures. Sandstones, shales and coal measures above

the Upper Limestone are largely eroded and are preserved only as large basinal outliers. Most of the Central Plain is underlain by Carboniferous carbonates, mainly the Lower and Middle Limestones.

The Lower Limestone Shales consist of alternating sandstones and shales passing upward into alternating dark limestones and shales. Its thickness, although variable over broad areas, probably averaged less than 200-300 feet. Lower Limestone Shales are overlain by muddy bioclastic limestones and minor dolomite of the Lower Limestone division. The Lower Limestone attains a thickness in excess of 1,000 feet over most of the Central Plain. Bioclastic carbonates of the Lower Limestone pass upward into a calcareous, bryozoan-brachiopod, mud bank complex termed the Waulsortian "reef" facies. The Waulsortian facies is believed to have occupied a broad area of about 3,000 square miles analogous to a barrier reef which separated deep water shales of the incipient Variscan geosyncline to the south from lagoonal limestones (Calp) to the north. The Waulsortian is diachronous. It developed first in the south where it attains its maximum thickness (2,500 feet near Limerick) and spread northward toward the latitude of Tynagh (500 feet thick). To the north Waulsortian knolls occur at several stratigraphic levels within the Calp.

The Calp or Middle Limestone consists of massive

bedded, black, non-fossiliferous limestones and shales with thin pyritic shale beds and contains banded and nodular cherts. It lies above and is in part equivalent to the Waulsortian.

The Upper Limestone is predominantly a bioclastic limestone. It is preserved only locally. In the vicinity of Galway Bay, Upper Limestone lies directly on Lower Limestone and this may be due to non-deposition as a result of Lower Carboniferous earth movements. The Carboniferous stratigraphy at the Mogul, Tynagh, Gortdrum and Riofinex mines together with ages and faunal zones of the various stratigraphic divisions is given in Figure 1.2.

Lower Carboniferous volcanic activity took place at a number of widely separated centres within the Central Plain. Most notable of these is the Pallas Hills southeast of Limerick where a graded series of basaltic lavas and tuffs is found at two horizons, lower and upper Viséan. The lavas include olivine basalts, trachybasalts, trachyandesites, trachytes and picrite basalts and are associated with tuffs and agglomerates, plugs and sills (Ashby, 1939). Carboniferous rocks are poorly exposed in Ireland and other volcanics doubtless exist beneath the cover of glacial drift and bog.

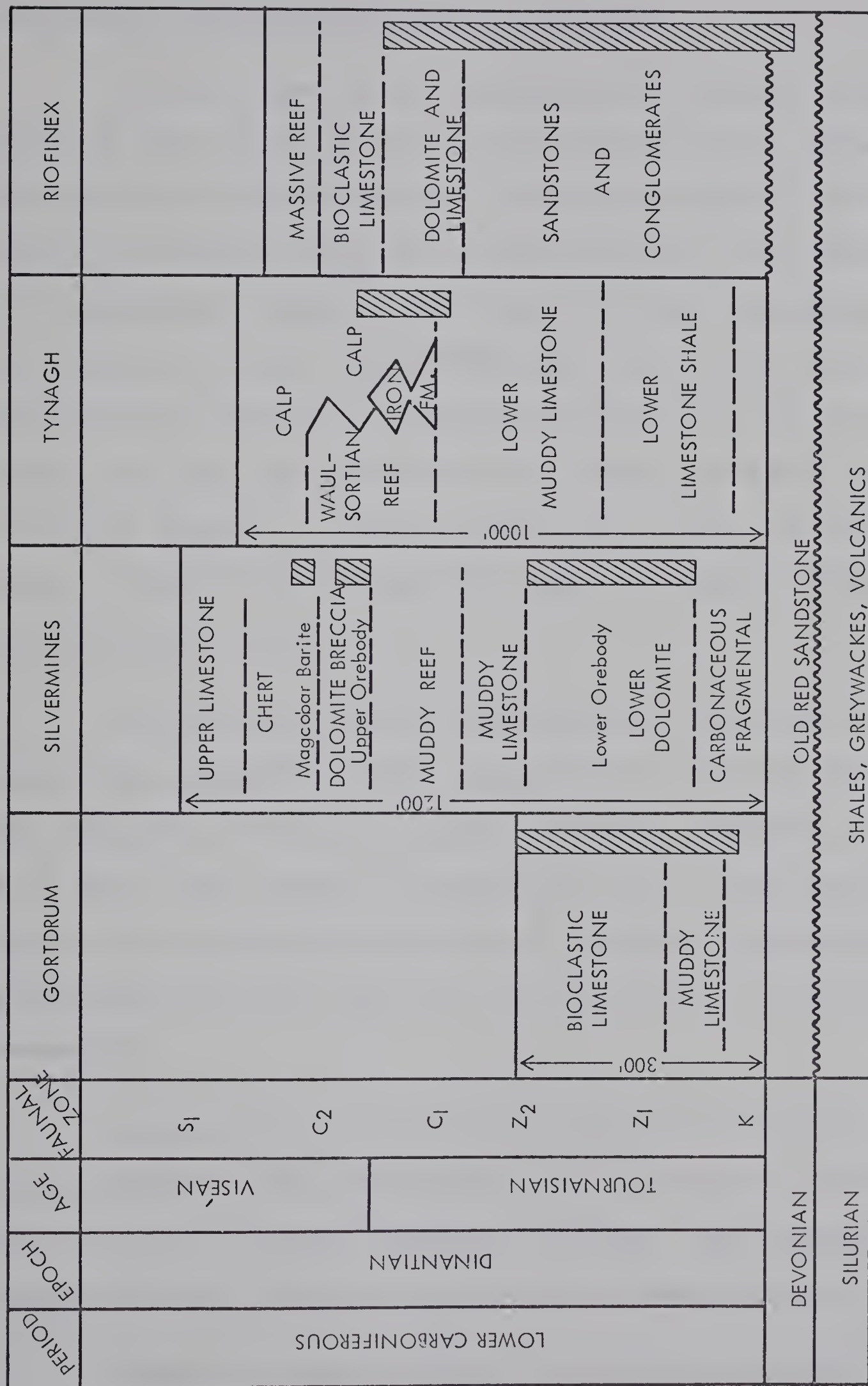


Fig. 1.2 Carboniferous stratigraphy and ore horizons at Mogul, Tynagh, Gortdrum and Riofinex mines (from Snelgrove, 1966)

Armorican (Permo-Carboniferous) Structure

At the close of the Carboniferous, intense folding, faulting and uplift of the Variscan geosynclinal sediments by Armorican stresses resulted in the development of the Hercynian mountain belt in southern Ireland. The intensity of deformation increases from north to south approaching the Hercynian front. Open folds and a few thrust faults characterize Armorican compressive stresses in the area of study, and with few exceptions the strata are flat lying to gently dipping. A major thrust fault marks the Hercynian front. South of this front the rocks are tightly folded and strongly cleaved.

Within and close to the Hercynian fold belt the structural alignment is EW. Progressing northerly from the Hercynian front the alignment changes gradually from E to ENE. This change in structural trend is believed due to the increasing influence of Caledonian basement structures which may have been reactivated by Hercynian movements.

Large inliers of Devonian sandstone and Silurian slate protrude above the Central Plain and appear to have been uplifted by broad Hercynian folding. The irregular shapes of these inliers suggest some basement control.

Numerous normal faults, the majority of which

strike ENE, may have developed in response to a relaxation of Armorican compressive stresses. The major movement on these faults would appear to have developed in a late Hercynian structural phase. Movement may have taken place along these faults in Lower Carboniferous times, however the evidence at hand is equivocal. The Mogul, Tynagh, Gortdrum, Riofinex and Tara base metal deposits are spatially related to ENE striking normal faults.

Post-Carboniferous

Permian through Triassic, Jurassic and Cretaceous sediments are preserved in northeast Ireland beneath a capping of Tertiary flood basalts. Permian strata may have been restricted to the northeast. The Mesozoic rocks on the other hand likely extended over all of Ireland and are now absent through erosion. The Tertiary basalts were probably largely restricted to their present distribution. These basalts represent the latest phase of igneous activity in Ireland.

Geology of the Base Metal Deposits

Consolidated Mogul Mine

Two distinct ore zones lie within Lower Carboniferous carbonates on hangingwall side of the Silvermines Fault (Figure 1.3). The Silvermines Fault strikes ENE,

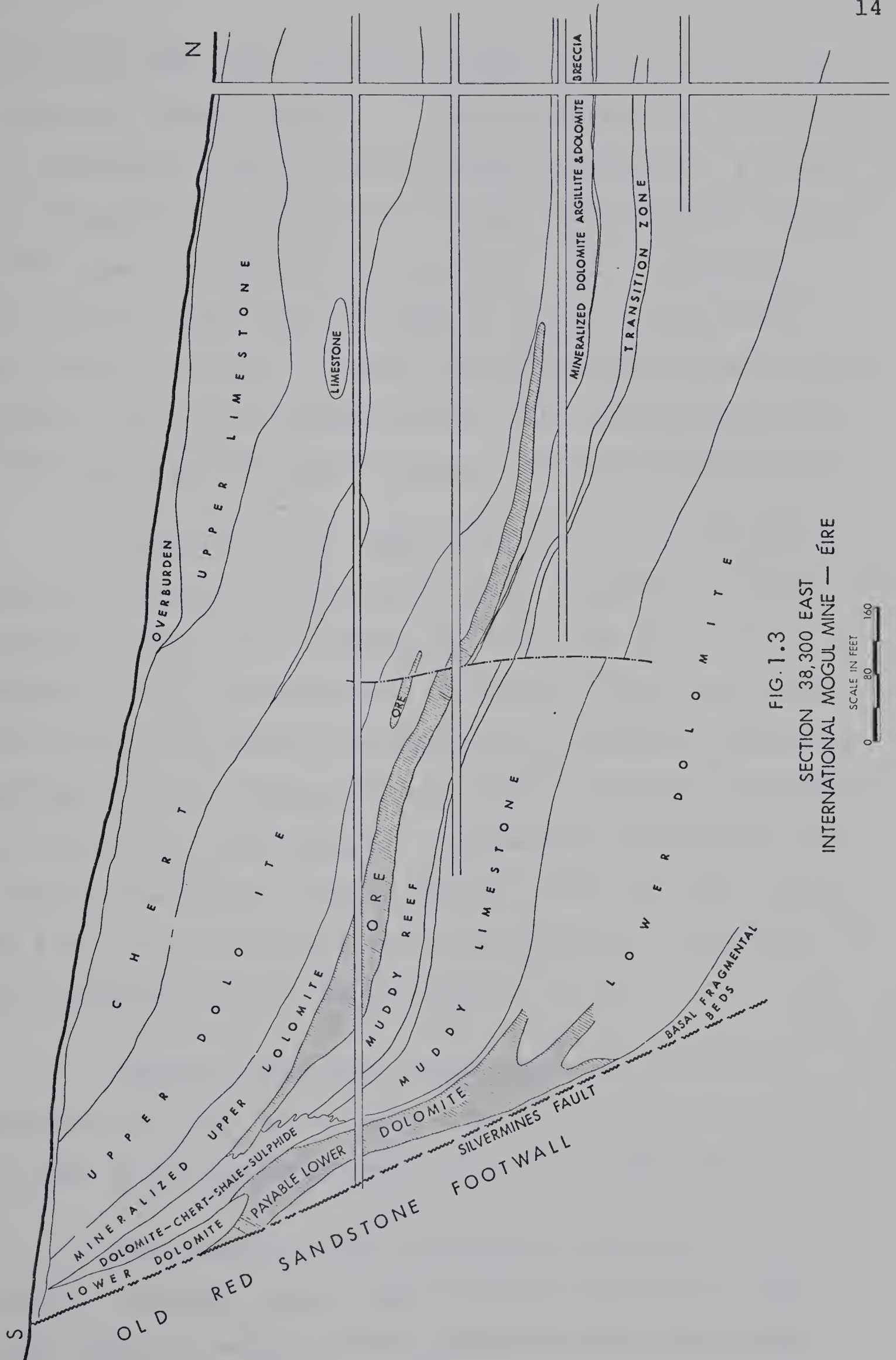


FIG. 1.3
SECTION 38,300 EAST
INTERNATIONAL MOGUL MINE — ÉIRE

dips about 65° north and has a normal displacement of 800-1100 feet (Rhoden, 1958). It marks the northern boundary of a Devonian inlier, the Silvermines Mountains. A lower discordant and disseminated ore zone (20% sulphides, Weber 1966) lies sub-parallel to the fault, and a stratiform and massive upper ore zone dips at $10-15^{\circ}$ to the north away from the fault. A large stratiform deposit of cryptocrystalline barite (Magcobar Mine) lies stratigraphically above the upper ore zone in upper dolomite of Viséan age.

Sulphides of the upper zone are almost exclusively microcrystalline, characteristically colloform and framboidal, pyrite (75%), sphalerite (20%) and galena (5%) (Weber, 1966). In contrast, sulphides of the lower zone are coarse grained and mineralogically diverse. According to Weber (1966), sphalerite and galena dominate and pyrite is accessory. Chalcopyrite, tetrahedrite, bournonite and arsenopyrite occur in minor amounts. The lead-zinc ratio is 1:4 in the stratiform ore and this ratio is reversed in the disseminated ore (Weber, 1966).

Numerous small base metal deposits occur for a distance of three miles along the Silvermines Fault and through a stratigraphic range of at least 500 feet.

The genesis of the Silvermines sulphides is controversial. Rhoden, whose study predates discovery of the Mogul deposit, believes that sulphide occurrences along

the fault are epigenetic hydrothermal. As evidence he states that mineralization postdates major fault displacement which he has shown to be at least post-Lower Carboniferous. He believes that metalliferous solutions were channeled along the fault and notes that bleaching and sulphidation of the Old Red Sandstone can be traced some distance from the fault. Although direct evidence is lacking he is of the opinion that the mineralization is Triassic to Jurassic in age.

Graham (1970) who has carried out detailed mineralogical studies of the Mogul deposit believes the lower orebody is epigenetic and the upper orebody is syngenetic. He believes that thermal connate waters leached base metals from lower Paleozoic rocks and were channeled upwards along the Silvermines Fault. On reaching the surface the sulphides were chemically precipitated in a restricted basin or lagoon. Evidence for a syngenetic genesis of the upper ore includes shape, conformable nature, colloform textures and structures resembling slump features in the upper ore and the pronounced mineralogical differences between the upper and lower orebodies.

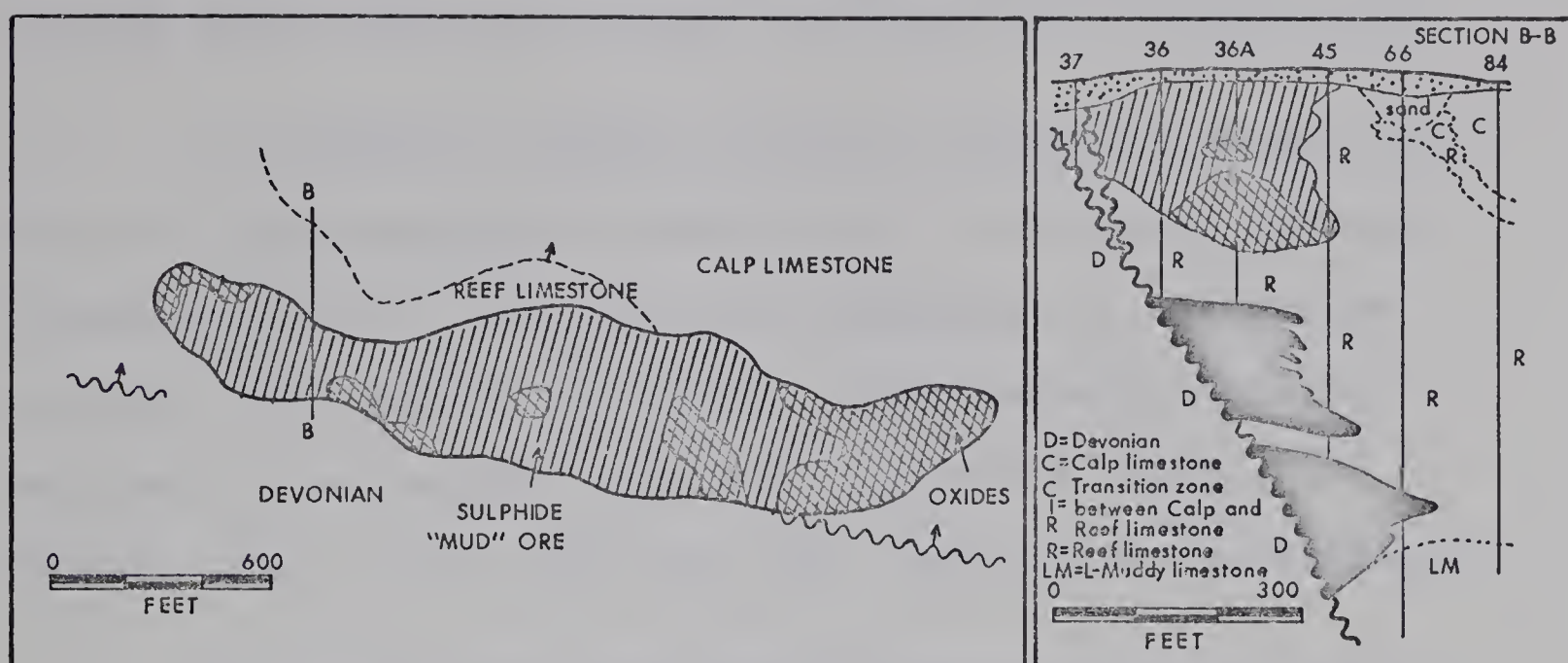
The stratigraphic position of the Mogul, Tynagh, Gortdrum and Riofinex mineralization in relation to local Carboniferous lithologies is given in Figure 1.2.

Tynagh Mine

The Tynagh lead-zinc-copper-silver orebody lies mainly within Waulsortian reef limestones on the north or hangingwall side of the North Tynagh Fault (Figure 1.4). The North Tynagh Fault strikes ENE and dips to the north at about 50° (Derry et al., 1965). In the vicinity of the mine a displacement of about 1,200 feet on the fault has juxtaposed Devonian Old Red Sandstone and Lower Carboniferous carbonates. Although the ore is contained mainly within the Waulsortian facies, mineralization in Carboniferous lithologies is known to extend over a length of 10,000 feet along the fault and through a stratigraphic thickness of 1,500 feet (Morrissey et al., 1968). Sulphides in uneconomic quantities are also found in the footwall sandstones. An iron formation which attains a maximum thickness of about 150 feet lies to the north of the orebody at the same stratigraphic level. The iron formation consists of banded hematite and chert and was probably chemically precipitated in a small restricted marine basin (Shultz, 1966a). A tuffaceous bed 5 feet thick was found in the mine area.

The primary sulphides are pyrite, sphalerite, galena and chalcopyrite in that order of abundance. Gangue is predominantly barite (up to 40%) and in part calcite. The sulphides occur as replacements and in-

(a)



(b)

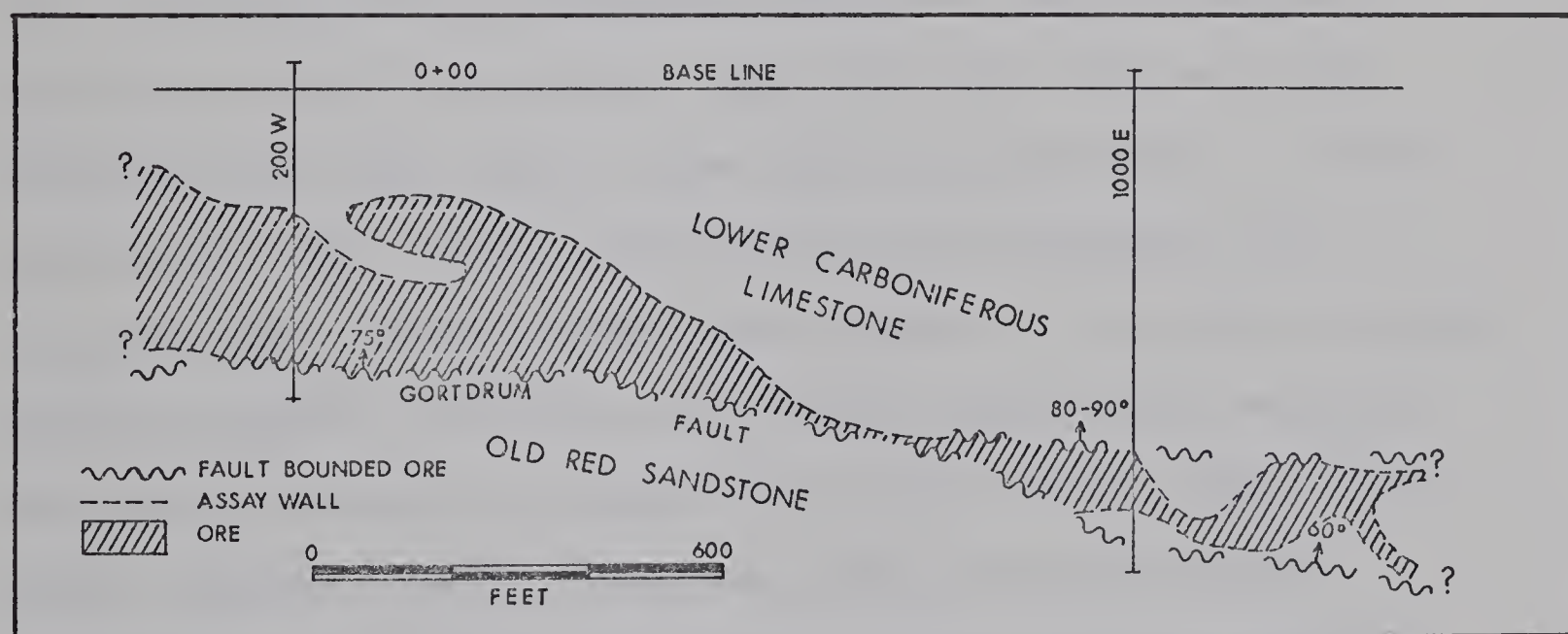


Fig. 1.4 (a) Plan and cross section of Tynagh deposit (from Derry, Clark & Gillatt, 1965)

(b) Plan of Gortdrum deposit (from Thompson, 1967)

fillings in fractured and brecciated reef limestones. The average ratio lead-zinc-copper is about 8:8:1 respectively.

A secondary orebody of black sulphide-rich mud lies atop the aforescribed primary ore. It contains economic concentrations of lead and zinc sulphides and carbonates together with pyrite and barite. This secondary ore is believed to be largely residual. Pieces of Sequoia and Cypress found in the mud date this residual ore as Tertiary.

The genesis of the Tynagh deposit is controversial. Derry et al., 1965 tentatively conclude that the primary ore "resulted from sulfataric solutions issuing during a period of local vulcanicity from fissures that may have followed the same zone as the North Tynagh Fault." These solutions, they state, precipitated the sulphides "by seeping into a reef or mud bank complex in an area of recent organic growth." The iron and silica remained in solution and precipitated in a restricted basin off the edge of the reef. Shultz, 1966b, disagrees with a penesynthetic formation. He emphasizes that the stratigraphic range of mineralization spans the entire Lower Carboniferous locally and that the major dimensions of mineralization parallel the plane of the fault. He produced evidence that the mineralization is post-faulting and that there is no support for the existence of the North Tynagh Fault in Lower

Carboniferous times. The iron formation he believes to be unrelated to the sulphide deposits. Shultz favours an epigenetic hydrothermal genesis.

Gortdrum Mine

Gortdrum deposit occurs in Tournaisian carbonates on the hangingwall side of an ENE striking normal fault (Figure 1.4). The footwall of the fault is Old Red Sandstone. An account of the Gortdrum deposit has been published by Thompson (1967). Ore minerals consist of barite, chalcopyrite, tetrahedrite and chalcocite which occur as disseminations and fracture fillings in dolomitized limestone and shaly limestone host rocks. The gangue is barite, calcite and dolomite. The axis of mineralization is subparallel to the fault and the tenor of the ore decreases with distance from the fault. Reserves are four million tons grading 1.2% copper and 0.75 ounces silver per ton. Thompson believes that hydrothermal solutions with a possible common origin to basic dykes in the area (likely related to Carboniferous volcanics of the Pallas area to the west) introduced the copper and silver minerals into already dolomitized and fractured host rocks.

Riofinex Mine

Sphalerite and galena together with minor amounts of

pyrite and barite occur in sandstones, conglomerates, shales and limestones adjacent to an EW striking fault. The host rocks range from Silurian through Devonian to Tournaisian and the mineralization spans a stratigraphic range of about 1,000 feet (Snelgrove, 1966). Mineralization is known to extend for six miles along the fault. However, the north-south extent is generally less than 150 feet (Morrissey et al., 1968). The fault is believed to postdate the youngest rocks preserved in the area.

Minor Base Metal Occurrences

Lead isotope ratios were determined for galenas from another 20 base metal occurrences shown in Figure 1.1. Four of these are veins in Silurian or Devonian sandstones and the remainder are disseminations, replacements and fracture fillings at various stratigraphic levels in the Lower Carboniferous. The mineralogy, host rocks and apparent controls are tabulated for each occurrence in Appendix 1.

CHAPTER II

THEORY

Introduction

Model lead interpretations are based on the ratios of the lead isotopes Pb^{204} , Pb^{206} , Pb^{207} and Pb^{208} in common lead. All lead has evolved by the addition of radiogenic Pb^{206} , Pb^{207} and Pb^{208} , which is produced by the radioactive decay of uranium and thorium, to an original or "primeval" lead, which existed at the time of formation of the earth (time of formation of the earth = t_0). Pb^{204} is non-radiogenic and its absolute abundance in the earth has not changed since the time t_0 . Common lead is lead which was isolated from uranium and thorium at the time of its mineralization (time of mineralization = t_1) and has subsequently remained free of uranium and thorium to the present time designated $t = 0$. Because the isotope ratios in common lead (uranium and thorium free by definition) cannot have changed since the time t_1 , these ratios are therefore identical to the isotopic composition of lead in the source region at the time t_1 .

The radiogenic lead isotopes are the stable decay

products of U^{238} , U^{235} and Th^{232} produced according to the following decay schemes.

<u>Parent Nuclide</u>	<u>Stable Decay Products</u>	<u>Half Life</u> <u>$\times 10^9$ years</u>
U^{238}	$Pb^{206} + 8 \text{ He} + \text{energy}$	4.49 ± 0.02
U^{235}	$Pb^{207} + 7 \text{ He} + \text{energy}$	0.713 ± 0.16
Th^{232}	$Pb^{208} + 6 \text{ He} + \text{energy}$	13.9 ± 0.03

The isotope ratios of any common lead whatsoever are defined exactly by the integral equations

$$x = a_o + \int_{t_1}^{t_o} \mu e^{\lambda t_1} \lambda dt$$

$$y = b_o + \int_{t_1}^{t_o} \nu e^{\lambda' t_1} \lambda' dt$$

$$z = c_o + \int_{t_1}^{t_o} w e^{\lambda'' t_1} \lambda'' dt \quad 2.1$$

provided that all lead was derived from primeval lead of abundances a_o , b_o and c_o . The symbols used in equations 2.1 are defined in Table 2.1.

Models for the Interpretation of Common Lead Isotope Ratios

Equations 2.1 cannot be used as such to date a common lead. Models must be constructed based on assumptions regarding the parameters μ , ν and w . The value of t_o must be known and depending on the model it may be necessary to know a_o , b_o and c_o .

TABLE 2.1

Symbols and Constants Used in Age Determination

Isotope Ratio	Present $t = 0$	Time t_1	Primeval $t = t_0$
$\text{Pb}^{206}/\text{Pb}^{204}$	a	x	a_0
$\text{Pb}^{207}/\text{Pb}^{204}$	b	y	b_0
$\text{Pb}^{208}/\text{Pb}^{204}$	c	z	c_0
$\text{U}^{238}/\text{U}^{235}$	137.8		3.33
$\text{U}^{238}/\text{Pb}^{204}$	μ	$\mu e^{\lambda t_1}$	$\mu e^{\lambda t_0}$
$\text{U}^{235}/\text{Pb}^{204}$	v	$v e^{\lambda' t_1}$	$v e^{\lambda' t_0}$
$\text{Th}^{232}/\text{Pb}^{204}$	w	$w e^{\lambda'' t_1}$	$w e^{\lambda'' t_0}$

<u>Parent Atom</u>	<u>Decay Constant in 10^{-9} yr.^{-1}</u>
U^{238}	$\lambda = 0.1537$
U^{235}	$\lambda' = 0.9722$
Th^{232}	$\lambda'' = 0.0499$

Geophysical constants	$t_0 = 4.578 \times 10^9 \text{ yr} -$ Cooper <u>et al.</u> , 1969
	$a_0 = 9.346.$ - Oversby, 1970
	$b_0 = 10.218$
	$c_0 = 28.96$

Gerling (1942), Holmes (1946) and Houtermans (1946) assumed that the ratios U^{238}/Pb^{204} , U^{235}/Pb^{204} and Th^{232}/Pb^{204} changed only by radioactive decay, in locally closed systems, during the time interval between t_0 and t_1 . Isotopic fractionation of uranium in nature is extremely rare, therefore the ratio U^{238}/U^{235} changes only by radioactive decay. The present day value of the ratio U^{238}/U^{235} or μ/V is 137.8. Assuming the above ratios change only by radioactive decay, equations 2.1 simplify to

$$x = a_0 + \mu(e^{\lambda t_0} - e^{\lambda t_1}) \quad (a)$$

$$y - b_0 + \frac{\mu}{137.8} (e^{\lambda' t_0} - e^{\lambda' t_1}) \quad (b)$$

$$z = c_0 + W (e^{\lambda'' t_0} - e^{\lambda'' t_1}) \quad (c) \quad 2.2$$

The ratio μ may be eliminated between equations 2.2 (a) and 2.2 (b) to give

$$\emptyset = \frac{y - b_0}{x - a_0} = \frac{(e^{\lambda' t_0} - e^{\lambda' t_1})}{137.8 (e^{\lambda t_0} - e^{\lambda t_1})} \quad 2.3$$

The right hand side of equation 2.3 is a constant for all leads mineralized at time t_1 . On a plot of y vs x , all leads mineralized at time t_1 will fall on a straight line through a_0 and b_0 and having slope \emptyset . This equation, known as Houtermans' "isochron equation", can be solved for t_1 , knowing only t_0 .

In subsequent years it was demonstrated that many ore leads of different ages, irrespective of geographic location, plot close to a single "growth curve" on graphs of y vs. x and z vs. x (Collins, Russell and Farquhar, 1953; Russell and Allan, 1954; and Russell and Farquhar, 1960a and 1960b).

With steady improvements in analytical techniques it became evident that most of the scatter in the earlier data, away from a single growth curve, could be attributed to experimental error and the lack of standardization. The remaining scatter was due mainly to the inclusion of a large number of anomalous leads which are discussed in a later section. The close approximation of many leads the world over to a single growth curve (Figure 2.1) cannot be explained if the lead has evolved in discrete systems, each with different U/Pb and Th/Pb ratios, as per the assumptions of Houtermans. They assumed, therefore, that many common leads have evolved from the time t_0 to the time t_1 , in a single closed system, homogeneous with respect to the ratios μ and W . These common leads which evolved in such a single homogeneous closed system became known as ordinary leads as opposed to anomalous leads which have a multi-stage history. The most likely source region for ordinary leads was considered to be the mantle. It was then possible to determine the values μ and W for the

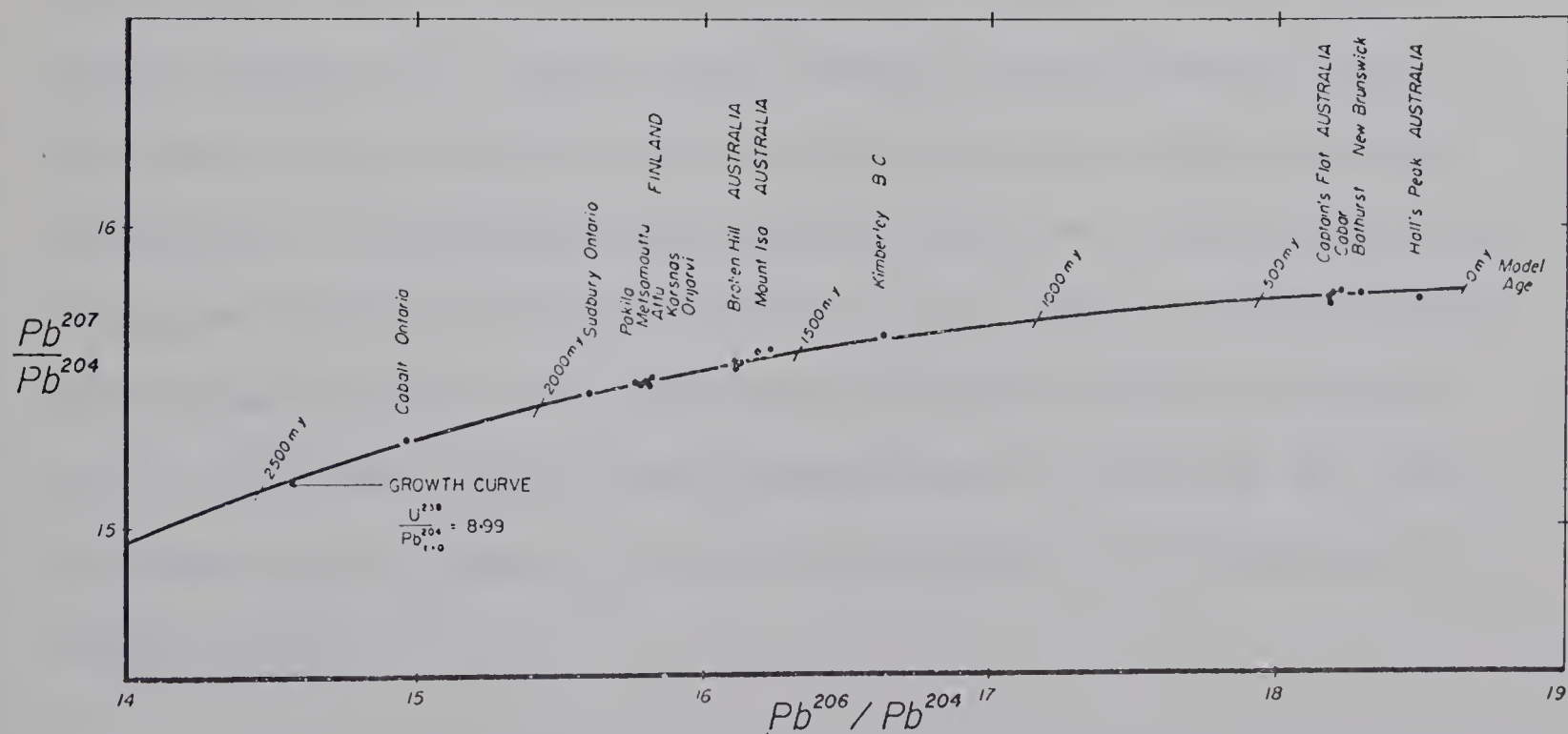
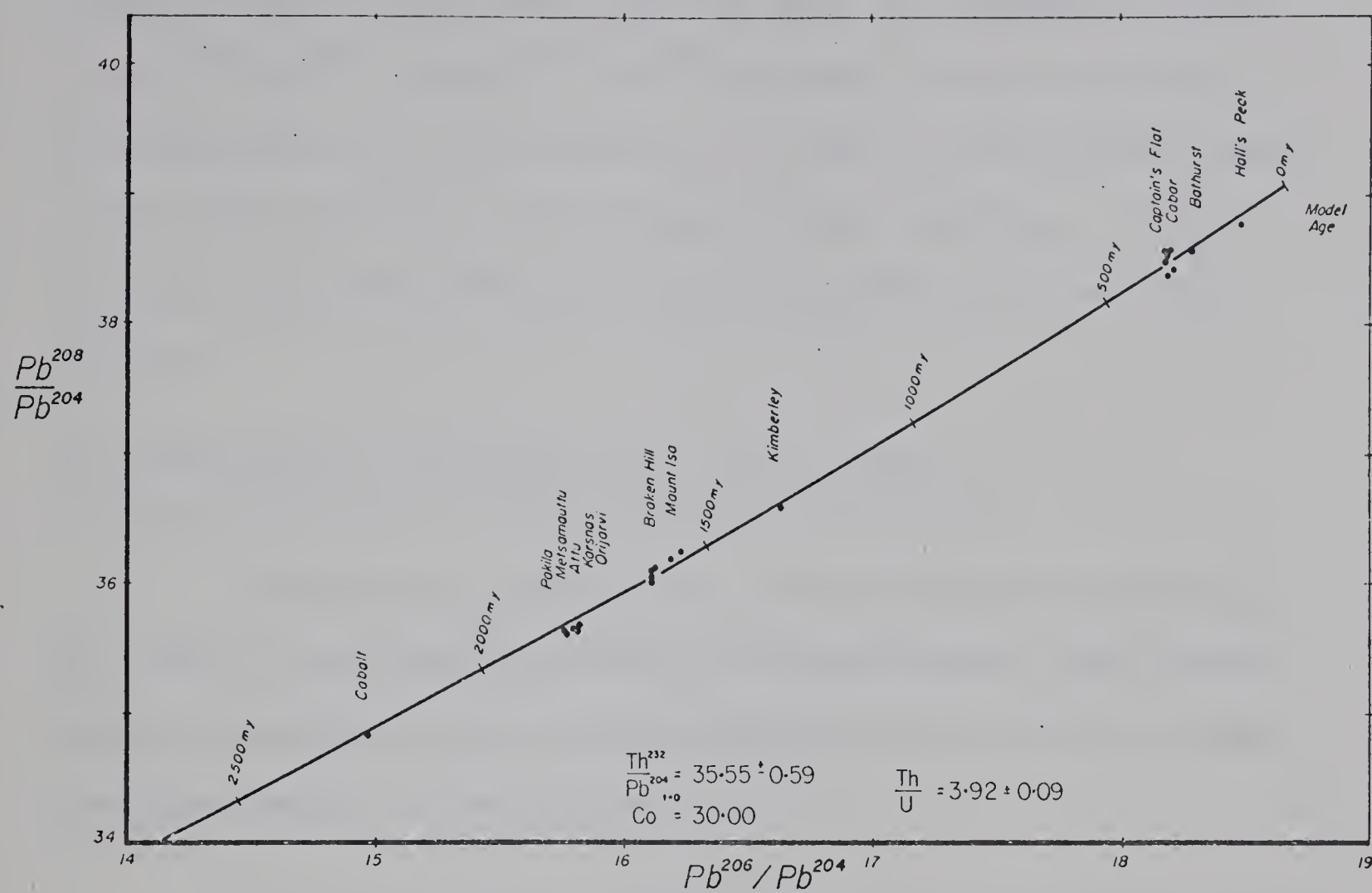


Fig. 2.1 Pb^{207}/Pb^{204} - Pb^{206}/Pb^{204} and Pb^{208}/Pb^{204} - Pb^{206}/Pb^{204} plots showing the close fit of many ore leads to a single growth curve (from Kanasewich and Farquhar, 1965).

growth curves which best fit the data and thereby relate the $U^{238}\text{-Pb}^{206}$ and $Th^{232}\text{-Pb}^{208}$ systems. With accurate determination of the ratios a_o , b_o and c_o of primeval lead (see next section), and the age of the earth t_o , it was possible to date ordinary leads on graphs of y vs x and z vs x .

The Geophysical Constants a_o , b_o , c_o and t_o

Precise knowledge of t_o , in particular, and of a_o , b_o and c_o is a prerequisite to accurate model lead dating. These constants have been determined by the study of lead isotope ratios in meteorites.

Patterson (1953) determined the lead isotope ratios in the troilite phase of two meteorites, Canyon Diablo and Henbury. The troilite in each case contained only negligible amounts of uranium and thorium, therefore the lead ratios had not changed measurably since the time of their formation. Averaging the ratios in the two meteorites, he obtained 9.50, 10.36, 29.49 for a_o , b_o and c_o respectively. Houtermans (1953) and Patterson (1953 and 1955) obtained 4.5×10^9 year for t_o using equations 2.2 (a) and 2.2 (b), assuming a_o , b_o and c_o to be the same for the earth as for meteorites.

Patterson (1956) showed that the lead isotope ratios

of three stone meteorites and two iron meteorites defined a straight line on a plot of y vs x and this line he called the "primary isochron" for $t = 0$. This showed that these meteorites are related through common values of a_0 , b_0 and c_0 , and proved that the lead ratios had developed from a common time t_0 in closed systems. The time t_0 was found to be $4.55 \pm 0.07 \times 10^9$ year, by applying the Houtermans isochron equation to the meteorite isochron. Patterson in the same publication showed that lead from modern galenas and from oceanic sediments plotted within the limits of error of the primary isochron, demonstrating quite conclusively a common time of origin for the earth and meteorites.

Several revisions in the values for a_0 , b_0 , c_0 and t_0 have been made subsequently using Patterson's method. The currently most accepted value for t_0 is 4.578×10^9 years (Cooper et al., 1969), which value is based on a new single-stage growth curve defined by more accurate ratios for a_0 , b_0 and c_0 (Oversby, 1970) and more precise measurements on ordinary leads (Cooper et al., 1969). The above ratios were determined more accurately by correcting for mass dependent and hence weighted fractionation. The newly revised values for a_0 , b_0 and c_0 are 9.346, 10.218 and 28.96 respectively.

Anomalous Leads

Leads which have developed in more than one closed U - Th - Pb system are called anomalous leads.

On the assumption of a single growth curve, all anomalous leads are a mixture of ordinary lead with lead produced in one or more different U - Th - Pb environments, with one exception. A mixing of two or more ordinary leads of different ages will produce an anomalous lead. In this instance, each of the end members has evolved in the same U - Th - Pb system but for different lengths of time. Anomalous leads which are not a mixing of ordinary leads can be defined by the general equation

$$x = a_0 + \mu(e^{\lambda t_0} - e^{\lambda t_1}) + \mu_1(e^{\lambda t_1} - e^{\lambda t_2}) + \mu_2(e^{\lambda t_2} - e^{\lambda t_3}) + \dots + \mu_{n-1}(e^{\lambda t_{n-1}} - e^{\lambda t_n}) \text{ etc. for } y \text{ and } z \quad 2.5$$

for n stages each having a different ratio μ . Generally, anomalous leads from a limited geographic region show a linear relationship or "anomalous lead line" on plots of y vs. x and z vs. x provided that mixing of the two components has been incomplete. Anomalous leads may be classified into the following types:

- (1) Mixture of two ordinary leads
- (2) Two-stage anomalous lead
- (3) Short period anomalous lead

(4) Simple three-stage anomalous lead

(5) Higher order multi-stage lead

The anomalous lead line resulting from a mixing of two ordinary leads with different ages should intersect the single-stage growth curve at two points and not extend beyond it.

Many examples of two-stage leads are documented in the literature (Farquhar et al., 1957, Heyl et al., 1966 and Sinclair, 1966). For a two stage lead equations 2.5 reduce to

$$x = x_0 + \mu_1(e^{\lambda t_1} - e^{\lambda t_2}) \quad (a)$$

$$y = y_0 + \frac{\mu_1}{137.8}(e^{\lambda' t_1} - e^{\lambda' t_2}) \quad (b)$$

$$z = z_0 + W_1(e^{\lambda'' t_1} - e^{\lambda'' t_2}) \quad (c) \quad 2.6$$

Eliminating μ , between equations 2.6 (a) and 2.6 (b)

$$R = \frac{y - \bar{y}_0}{x - \bar{x}_0} = \frac{(e^{\lambda' t_1} - e^{\lambda' t_2})}{137.8(e^{\lambda t_1} - e^{\lambda t_2})} \quad 2.7$$

where \bar{x}_0 , \bar{y}_0 and z_0 are the average isotope ratios of the ordinary lead component (Kanasewich, 1962b). The ratios \bar{x}_0 and \bar{y}_0 are given by the point of intersection of the anomalous lead line with the growth curve, and from these, t_1 can be calculated and equation 2.7 solved for t_2 . Alternatively, uncontaminated ordinary leads may be found and from these \bar{x}_0 and \bar{y}_0 measured directly. Similarly t_2 may

be determined on a plot of z vs. x .

Two-stage leads where the second stage is relatively short are called short period anomalous leads. The anomalous lead line is almost tangent to the growth curve. The length of the anomalous lead line depends upon the U/Pb ratios, the duration of the second stage and the degree of homogenization prior to the time of mineralization. Great precision in the data is required in order to recognize a short period anomalous lead line and determine its slope.

Some anomalous leads have been interpreted as three stage (Ulrych, 1964), however because of the complexities of multistage leads, mathematical and geological interpretation is extremely difficult. It is believed that leads with histories of three or more stages are rare. Hypothetical three stage, six stage and eleven stage models have been considered by Kanasewich (1962b).

Other Models

Mantle Depletion Models

Uranium and thorium partition between crust and mantle so as to cause a depletion of these elements in the mantle. Models have been constructed, notably by Damon (1954) and Vinogradov et al. (1959), which account for the change of μ and W resulting from this depletion.

Mantle differentiation models vary on their assumptions of the rate of continental accretion and rate of convective turnover or homogenization of the mantle. The effect of this differentiation on the parameters μ and W is a subject of debate. Certainly differentiation does occur. On a consideration of relative volumes of crust and mantle (above 500 Km), and assuming the mantle is homogenized by convection, the resulting depletion of U and Th in the mantle must be minor.

Continuous Mixing Model

Armstrong (1968) has considered the case of continuous mixing of crust and mantle, which process tends toward isotopic equilibrium between the two environments. According to Armstrong, this would explain the lack of observed depletion of U and Th in the mantle.

Sedimentary Source Model

Tilton et al. (1965), Ulrych (1967) and Tatsumoto (1966a and 1966b) have shown from studies on rock leads that volcanic rocks of various island groups in the Pacific Ocean are inhomogeneous with respect to the ratios U:Th:Pb. These ratios are variable even within a geographically limited area such as a single island group. These authors believe that the observed isotopic heterogeneity is a result of derivation of the volcanics from an isotopically

heterogeneous upper mantle. Others believe the pattern is a result of crustal lead contamination of ordinary upper mantle lead. A study of U, Th and Pb isotope ratios in eclogite inclusions in kimberlites similarly suggests the mantle is heterogeneous (Lovering and Tatsumoto, 1968). The above considerations cast doubt on the assumption that the mantle is a direct source of ordinary leads.

Chow and Patterson (1959 and 1962) have shown that leads from modern pelagic sediments and manganese nodules, of both the Atlantic and Pacific, are isotopically uniform over extensive areas, and plot almost on a projection of the growth curve for ordinary leads. The μ and W/U ratios for these leads average about 9.00 and 4.14 respectively. Both ratios are in close agreement with the μ and W/U ratios for the source of ordinary leads.

The model ages are negative (in the future); about - 200m.y. for Pacific and - 400 m.y. for Atlantic leads. A part of the lead in these pelagic sediments has been derived through erosion of crustal rocks. An indeterminate but probably significant part has likely been derived directly from the mantle by exhalative processes. A large proportion of the lead derived through erosion must have been contributed by sialic rocks. Uranium and thorium are greatly enriched relative to lead in sialic as compared to basic rocks, and the comparatively radiogenic lead produced

in this environment would explain the observed negative age anomaly.

On a very general scale the amount of this negative anomaly is probably a function of the amount of sialic material exposed to erosion at any given time in the past. If the continents have been formed by a process of continental accretion, then the amount of sialic material exposed to erosion and hence the radiogenic component of oceanic lead, has increased with time. Even if continental accretion has not occurred, lead contributed to the oceans should become increasingly radiogenic with time due to the natural evolution of lead in a sialic environment characterized by high Th/Pb and U/Pb ratios. If this oceanic lead was remobilized to form a common lead, or lead ore, the amount of shift toward a younger model age for the ore would depend on its actual age of mineralization. This shift might not be noticeable for the oldest leads but may be quite pronounced for the more recently mineralized leads.

The $\text{Th}^{232}/\text{U}^{238}$ ratio (determined from the measured lead ratios) for oceanic leads is the average for the environment (the lead source) in which the leads evolved, and not for the sediment itself. If the $\text{Th}^{232}/\text{U}^{238}$ ratio in the sediments deviates significantly from this average ratio for the source in which the leads evolved, then given a suffi-

cient time lapse between formation of the sediment and removal of the lead to form ore lead (residence time), deviations from the single growth curve would be apparent on a plot of z vs. x .

Crustal Magmatic Source

The Th/U ratios in igneous rocks vary between wide limits, however the average ratio on a continental scale is about the same as that for the source of ordinary leads (Heier and Rogers, 1963). An apparently ordinary lead can only be derived from a magmatic environment if:

1. The magma was formed directly from a system having U^{238} and Th^{232} to Pb^{204} ratios equivalent to the source for ordinary leads, and soon after its formation lead in the granite was remobilized to form common lead.
2. The magma, by coincidence, happened to have the same U/Pb and Th/Pb ratios as the source for ordinary leads and the lead was remobilized to form a common lead at any time since.

There are several equally unlikely situations whereby an apparently ordinary lead could be derived from a crustal magmatic environment. These same considerations apply with

the necessary reservations to any geological environment.

Summary

There is some evidence that the upper mantle and lower crust is not homogenous with respect to the ratios U:Th:Pb. It has been demonstrated that leads from modern pelagic sediments are isotopically uniform over broad areas and plot on or close to the single-stage growth curve for ordinary leads. Also the W/ μ ratio for these leads is almost identical with that for the source of ordinary leads. Certain oceanic sediments may therefore constitute a source of apparently ordinary leads and the single-stage growth curve may define the average isotopic constitution throughout time of crustal and upper mantle lead introduced into the sea.

CHAPTER III

METHODS, ERRORS AND RESULTS

Sample Preparation

A total of 29 lead isotope determinations were made. In each case a microscopically pure galena separate was carried through a careful dithizone extraction procedure (Appendix 1) to ensure a pure sample. The end product of this procedure is about 50-100 μ g. of fine Pb sulphide, ready for loading on the mass-spectrometer filament.

Precautions were taken to prevent any contamination from any reagents or glassware used in the extraction procedure. Reagents were prepared from high purity components and then washed (with HCl or dithizone) to remove any traces of metals present. Glassware was cleaned in hot concentrated NaOH for at least 6 hours, rinsed with distilled water, cleaned again in hot concentrated HNO₃ for at least 6 hours, rinsed carefully with triple distilled water and then wrapped in parafilm.

Prior to loading a sample, the filament, which is made of pure tantalum ribbon, is outgassed at 4 Amps and for a minimum of 3 hours in a vacuum of 10^{-6} Torr. This

outgassing serves two purposes. It removes any lead contamination on the surface of the filament and changes the physical characteristics of the tantalum, which, by experience, produces a better run. The outgassed filament is loaded with 20-50ug. of the purified PbS and gradually heated at about 2 Amps and 15 Volts. This heating converts at least some of the PbS to fused PbO. The filament is then ready for mounting in the mass-spectrometer.

Analytical Methods and Instrumentation

Samples were run on a 12" radius, 90° sector, single filament, solid source mass-spectrometer, designed and built by Dr. G. L. Cumming of the Department of Physics, University of Alberta. In the mass-spectrometer, the samples were ionized at 1.6 to 2.0 Amps filament current in a vacuum of 5×10^{-8} atm. and accelerated to 4 KV. The current necessary to produce strong emission varied from one run to the next, depending on sample size and the amount of more volatile elements present. Simultaneous recordings of peak heights were made graphically on a chart recorder, and numerically on a digital voltmeter set to 1 second integration. The chart recorder was used for monitoring the stability during a run.

The mass-spectrometer measures the ratios 206/204

207/206 and 208/206. For a given ratio, eg. 206/204, a set of peaks were recorded in alternate fashion, eg. 206 - 204 - 206 - 204 etc., by the use of a switching mechanism. At a given filament setting the strength of emission is rarely constant. It may be either increasing or decreasing linearly and therefore the switching from one peak to the next was done at regular time intervals, usually of 12 or 15 seconds. At least 20 pairs, eg. 206 - 204, were determined for each of the three ratios at a given filament setting. After measuring the three ratios in the above fashion, the filament current was increased to produce stronger emission and the same procedure repeated. Normally each sample was run at three different filament settings, depending on the stability.

The most stable ratio sets for each filament setting were chosen from the chart recording. The corresponding numerical values from digital voltmeter print-out were used in the computations. The ratios corresponding to each filament setting were averaged to give the reported ratio.

Accuracy of Results

To properly appraise the reliability of the results, it is necessary to consider all the possible sources of error. Error can be attributed to Pb contamination and instrumentation error. These sources of error are examined

in turn.

Possible sources of contamination include reagents, glassware and filaments. The precautions taken to avoid contamination from reagents and glassware have been mentioned. Once cleaned these materials are tightly sealed to prevent contamination from atmospheric lead pollution. As a check, a blank was run through the complete extraction procedure using about 2 ml. of 0.001% dithizone. This is equivalent to a maximum of 0.8 μ g. of Pb. No colour change was observed and therefore the amount of contaminant Pb from reagents and glassware is much less than 0.8 μ g. Contamination is probably not greater than 0.1 μ g, thus for 100 μ g of Pb carried through the extraction procedure the contaminant would be about 0.1% by weight. The effect of 0.1% by weight of contaminant Pb on the measured ratios should be insignificant unless the isotope ratios of the contaminant Pb are in very different proportions than in the sample. The tantalum ribbon used for the filaments is essentially Pb free. Any trace amount of Pb on the surface of the filament should be removed by outgassing.

Instrumentation error is most serious. This is the product of fractionation in the mass-spectrometer, non-linearity of the recording apparatus, instability of the

run and inaccurate measurements of the Pb^{204} peak.

Isotopic fractionation in the mass-spectrometer seems to vary depending on the length of time a sample is run and the filament settings used. To minimize weighted fractionation, each sample was run at several different filament settings and the ratios for each setting were averaged. The error caused by non-linearity of the recording apparatus varies in inverse proportion to the peak height and results in a measured value lower than the true value. This error is most pronounced for the Pb^{204} peak. An examination of the 29 chart recordings reveals no definite correlation between the size of the Pb^{204} peak and the magnitude of the 206/204 ratio, either within a given sample run or between different samples. This error must be masked by other errors in the measurement of the Pb^{204} peak.

Normally variations due to instability of the mass-spectrometer are not weighted in either one direction or the other and can be compensated for by averaging a sufficiently large number of values. Only the stablest set of peaks, chosen on the basis of the best straight line fit, were used in the calculations. In cases of greater instability, the sample was rerun. The standard deviation for each ratio in Table 3.2 is a measure of instability only.

The most significant error occurs in measuring the small Pb^{204} peak because it is most susceptible to variations in background. An indication of the expected Pb^{204} error is afforded by the intercomparison standards given in Table 3.1. The 207/204 and 208/204 ratios are obtained by multiplying the 207/206 and 208/206 ratios by the 206/204 ratio and, therefore, the Pb^{204} error is transferred to these other ratios. All other errors are masked by Pb^{204} error. When plotted on a graph of y vs. x or z vs. x , samples with errors in the Pb^{204} abundances fall on a line between the origin and the point representing its true isotope ratio. These lines are called Pb^{204} error lines. On the graph of z/x vs. y/x (208/206 vs. 207/206), the Pb^{204} error is removed entirely (the directly measured ratios are used, not the ratios relative to Pb^{204}). Sample points on this type of plot should agree closely with the absolute values and the scatter should be a good measure of the geologic variation in the isotope ratios. Error lines in the latter case refer to Pb^{206} error.

A good test of the reliability of the mass-spectrometer is provided by the Broken Hill Intercomparison Standard and the Equal Atom Lead, NBS 982. The ratios and precisions of the two Pb standards are given in Table 3.1. Five runs of the equal atom standard were interspersed with sample runs as a check on mass-spectrometer performance. The precision of these runs is reported in Table 3.2.

TABLE 3.1

Calibration of the 12 Inch Mass Spectrometer with
NBS 982 and Broken Hill Leads (after Green, 1968)

NBS 982

	U. of A.	Stand values (Catanzaro <u>et.al.</u> , 1968)	Precision %
208/206	1.0001 ± 0.0005	1.0002	0.01
207/206	0.4671 ± 0.0002	0.4671	--
204/206	0.02717 ± 0.00003	0.02722	0.2

Broken Hill galena

	U. of A.	Ulrych (pers. comm. Baadsgaard, 1967)	Precision %
208/206	2.2282 ± 0.0010	2.2283	0.005
207/206	0.9616 ± 0.0010	0.9620	0.04
204/206	0.06239 ± 0.00004	0.06248	0.1

TABLE 3.2

CORRECTED LEAD ISOTOPE RATIOS

Sample No. Sequence No. ()				Sample No. Sequence No. ()			
206/204				207/204			
208/204				208/204			
1 (21)	18.11 ± 0.02	15.67 ± 0.02	38.23 ± 0.02	13C (18)	18.28 ± 0.02	15.62 ± 0.02	38.15 ± 0.02
2 (24)	18.26 ± 0.06	15.69 ± 0.06	38.51 ± 0.06	13D (33)	18.42 ± 0.02	15.77 ± 0.02	38.46 ± 0.02
3A (31)	18.04 ± 0.02	15.54 ± 0.02	37.83 ± 0.02	13E (19)	18.34 ± 0.02	15.70 ± 0.02	38.36 ± 0.02
3B (14)	18.11 ± 0.03	15.62 ± 0.03	38.06 ± 0.03	14 (6)	18.29 ± 0.04	15.64 ± 0.04	38.24 ± 0.04
4 (10)	18.19 ± 0.03	15.69 ± 0.03	38.32 ± 0.03	15 (13)	18.33 ± 0.02	15.67 ± 0.02	38.29 ± 0.02
5 (16)	18.28 ± 0.03	15.60 ± 0.03	38.15 ± 0.03	16 (2)	18.27 ± 0.03	15.63 ± 0.04	38.24 ± 0.03
6 (17)	18.29 ± 0.01	15.63 ± 0.01	38.11 ± 0.02	17 (8)	18.21 ± 0.02	15.54 ± 0.02	38.00 ± 0.02
7 (3)	18.24 ± 0.02	15.63 ± 0.02	38.30 ± 0.02	18 (27)	18.28 ± 0.02	15.63 ± 0.02	38.18 ± 0.02

TABLE 3.2, continued

Sample No. Sequence No. ()				Sample No. Sequence No. ()			
206/204				207/204			
208/204				208/204			
8 (32)	18.16 ± 0.02	15.57 ± 0.02	38.01 ± 0.02	19 (30)	18.32 ± 0.03	15.68 ± 0.03	38.40 ± 0.03
9 (15)	18.27 ± 0.02	15.68 ± 0.02	38.34 ± 0.02	20 (26)	18.31 ± 0.009	15.67 ± 0.01	38.30 ± 0.01
10 (12)	18.19 ± 0.04	15.58 ± 0.04	38.03 ± 0.04	21 (5)	18.20 ± 0.02	15.58 ± 0.02	37.98 ± 0.02
11 (34)	18.14 ± 0.02	15.52 ± 0.02	37.91 ± 0.02	22 (9)	18.24 ± 0.02	15.60 ± 0.03	38.21 ± 0.02
12 (25)	18.26 ± 0.02	15.67 ± 0.02	38.31 ± 0.02	23 (7)	18.26 ± 0.008	15.63 ± 0.008	38.27 ± 0.009
13A (20)	18.37 ± 0.03	15.72 ± 0.03	38.43 ± 0.03	24 (28)	18.19 ± 0.02	15.63 ± 0.02	38.21 ± 0.02
13B (23)	18.34 ± 0.02	15.70 ± 0.02	38.44 ± 0.02				

TABLE 3.2, continued

Interspersed Runs of Equal Atom Standard

NBS 982

Sequence	$\text{Pb}^{208}/\text{Pb}^{206}$	Precision*
1	$1.0006 \pm .005$.04%
4	$1.004 \pm .0008$.4%
11	$1.00007 \pm .0009$.02%
22	$1.0005 \pm .0006$.03%
29	$1.002 \pm .001$.2%

* Compared to accepted value of 1.0002

Results

Measured lead isotope ratios were corrected using the correction factors $206/204 = 0.99815$, $207/204 = 0.99723$ and $208/204 = 0.99630$ which are based on a large statistical population of intercomparison runs on the NBS 982 standard at the University of Alberta. Five runs of NBS interspersed with the 29 sample runs (Table 3.2) provide a measure of mass-spectrometer performance but are too few in number to allow calculation of statistically reliable correction factors.

The corrected lead isotope ratios together with standard deviations are presented in Table 3.2. These results are presented graphically on plots of y vs. x , z vs. x and z/x vs. y/x in Figures 4.2, 4.3 and 4.4.

CHAPTER IV

INTERPRETATION AND CONCLUSIONS

Growth Curves

Recently revised geophysical constants $a_o = 9.346$, $b_o = 10.218$ and $c_o = 28.96$ (Oversby, 1970) and age of the earth $t_o = 4.578 \times 10^9$ years (Cooper et al., 1969) were used in calculating the growth curves. The best fit growth curve on the plot of y vs. x was chosen to pass through the average of the data and has a μ (U^{238}/Pb^{204}) ratio of 8.79 (Figure 4.2). This growth curve happens to be the best fit growth curve (Cooper et al.) for ordinary or single-stage leads. Having determined the μ value for the best fit growth curve on the plot of y vs. x , the value of 36.4 for W (Th^{232}/Pb^{204}) was determined to position the growth curves through the average of the data on the plots of z vs. x (Figure 4.3) and z/x vs. y/x (Figure 4.4). Selection of the best fit growth curves was done by estimation, not mathematically. Error lines and isochrons are shown for various ages on the respective growth curves.

Errors

It is important to the interpretation to determine whether scatter in the data points on the graphs is real or

e 4

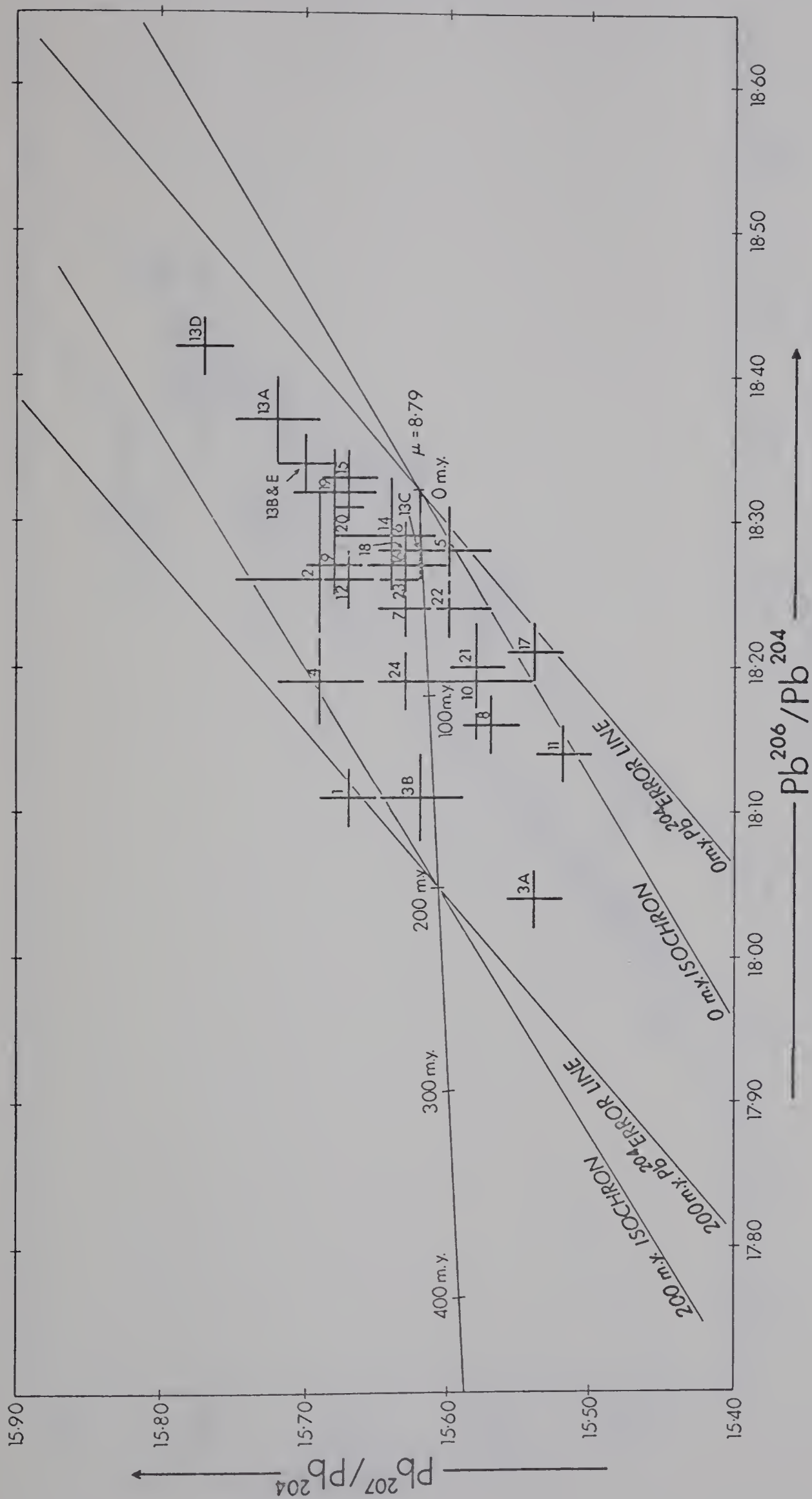


Fig. 4.2 Plot of Pb^{207}/Pb^{204} versus Pb^{206}/Pb^{204}

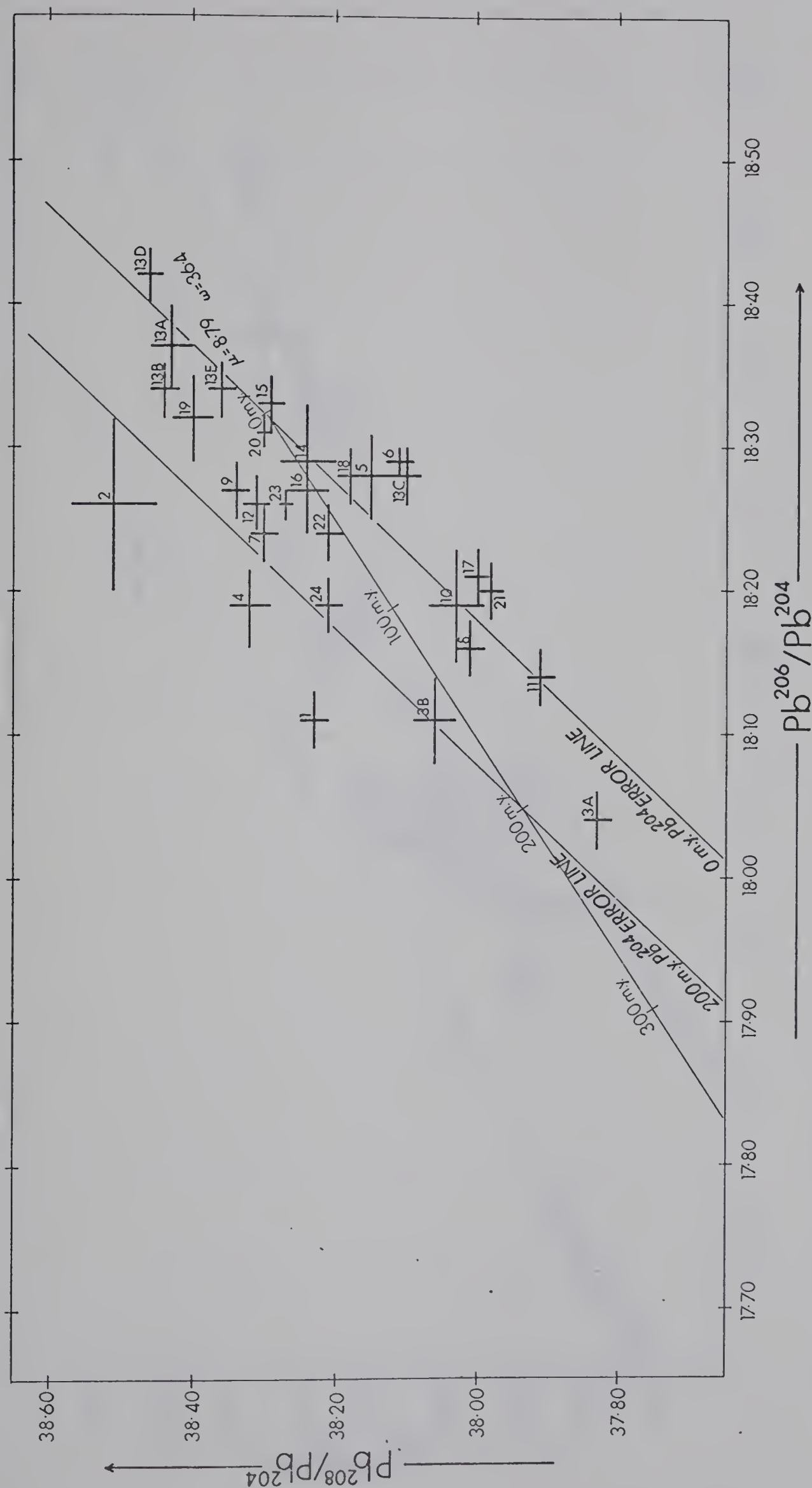


Fig. 4.3 Plot of Pb^{208}/Pb^{204} versus Pb^{206}/Pb^{204}

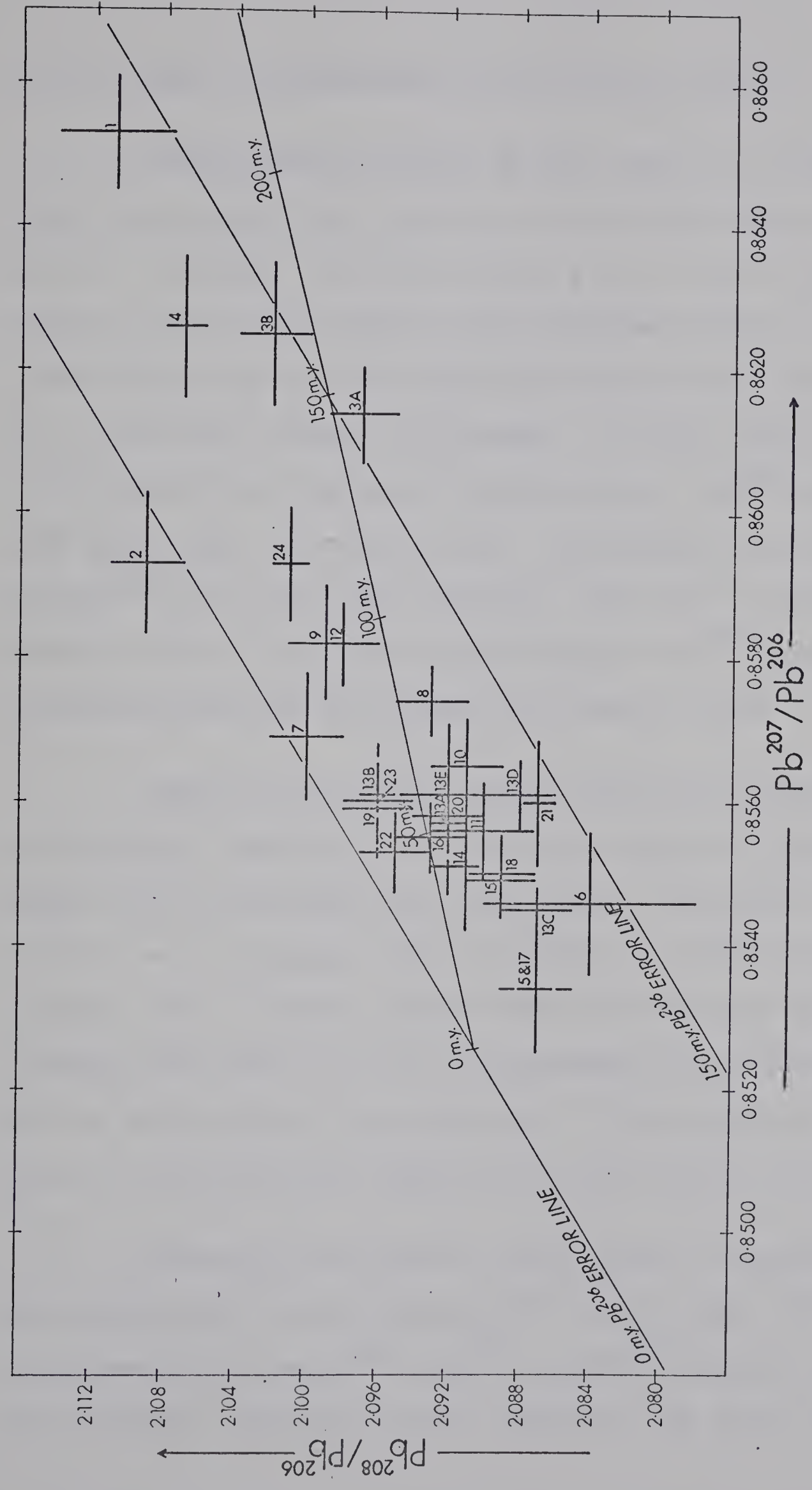


Fig. 4.4 Plot of Pb^{208}/Pb^{206} versus Pb^{207}/Pb^{206}

due to error in measurement of the lead ratios.

Considerable scatter in the ratios is evident on the y vs. x and z vs. x plots, and to some extent on the z/x vs y/x plot. On the plot of y vs. x all 29 points are within 0.9% of the growth curve measured along a Pb^{204} error line, and all but four are within 0.5%. On the z vs. x plot the scatter is greater. All but three points are within 1% of the growth curve along a Pb^{204} error line and about half are within 0.5%. On the z/x vs. y/x plot the Pb^{204} error has been removed. All but 4 points lie within 0.5% of the growth curve along a Pb^{206} error line and more than half the points lie within 0.25%.

Samples from three closely defined geographic areas, Silvermines (samples 13-20 inclusive) Tynagh (3 and 4) and Ennis (6-11 inclusive) are distributed linearly on the y vs. x and z vs. x graphs, almost parallel to Pb^{204} error lines (Figure 4.1). Scatter in the data is therefore probably largely the result of Pb^{204} measurement error although some may be due to mass fractionation. A similar error alignment is not nearly as apparent on the plot of z/x vs. y/x.

Although the largest errors would be expected in the measurement of the small Pb^{204} peak, some error in the measurement of the Pb^{206} , Pb^{207} and Pb^{208} peaks is likely, and probably accounts for the smaller, but still significant

spreads on the z/x vs. y/x plots.

Interpretation Based on Lead-Model

Single-Stage or Anomalous

Scatter in the ratios for samples from limited geographic areas is about parallel to error lines, and the observed error is within expected experimental error based on the error range in measurements of the NBS 982 standard. For these reasons it is likely that scatter is due to Pb^{204} error and/or mass fractionation. Taking into account the error spread, the data would group closely about the revised single-stage growth curve of Cooper et al. ($\mu = 8.79$). The Irish leads may therefore be interpreted as single-stage leads. This is readily apparent on the graph of y vs. x (Figure 4.5) which displays the entire growth curve of Cooper et al.

Alternatively, the Irish leads could be short period anomalous leads because of the large spread in the data in the direction of the Pb^{206}/Pb^{204} axis on the plot of y vs. x . A single short period anomalous lead line would indicate that the Irish leads were mineralized at the same time. Recognition of a short period anomalous lead line and mathematical interpretation in terms of a short period two-stage model however, would require at least an

order of magnitude greater precision in the data. The following discussion of source and model age is therefore limited to the former of the two possibilities, namely a single-stage interpretation.

Source of Leads, Single-Stage Model

According to a single-stage model, the lead evolved in an environment homogeneous throughout time with respect to the ratios U/Pb, Th/Pb and Th/U. The uniform source of the Irish leads has present ratios of $U^{238}/Pb^{204}=8.79$, $Th^{232}/Pb^{204}=36.4$ and $Th^{232}/U^{238}=4.14$.

Model Age, Single-Stage Model

The model age for a point which deviates from the growth curve because of measurement error can be determined by projecting the point to the growth curve along an error line. Similarly in the case of mass fractionation, the point is projected along a fractionation error line. The time of mineralization is then read directly off the growth curve.

The age of mineralization as determined on the plot y vs. x should be more accurate. Scatter is more clearly the result of Pb^{204} error. Also the angle of intersection between the Pb^{204} error line and the growth curve is more obtuse than on the z vs. x and z/x vs. y/x plots, where the error lines intersect the growth curves at

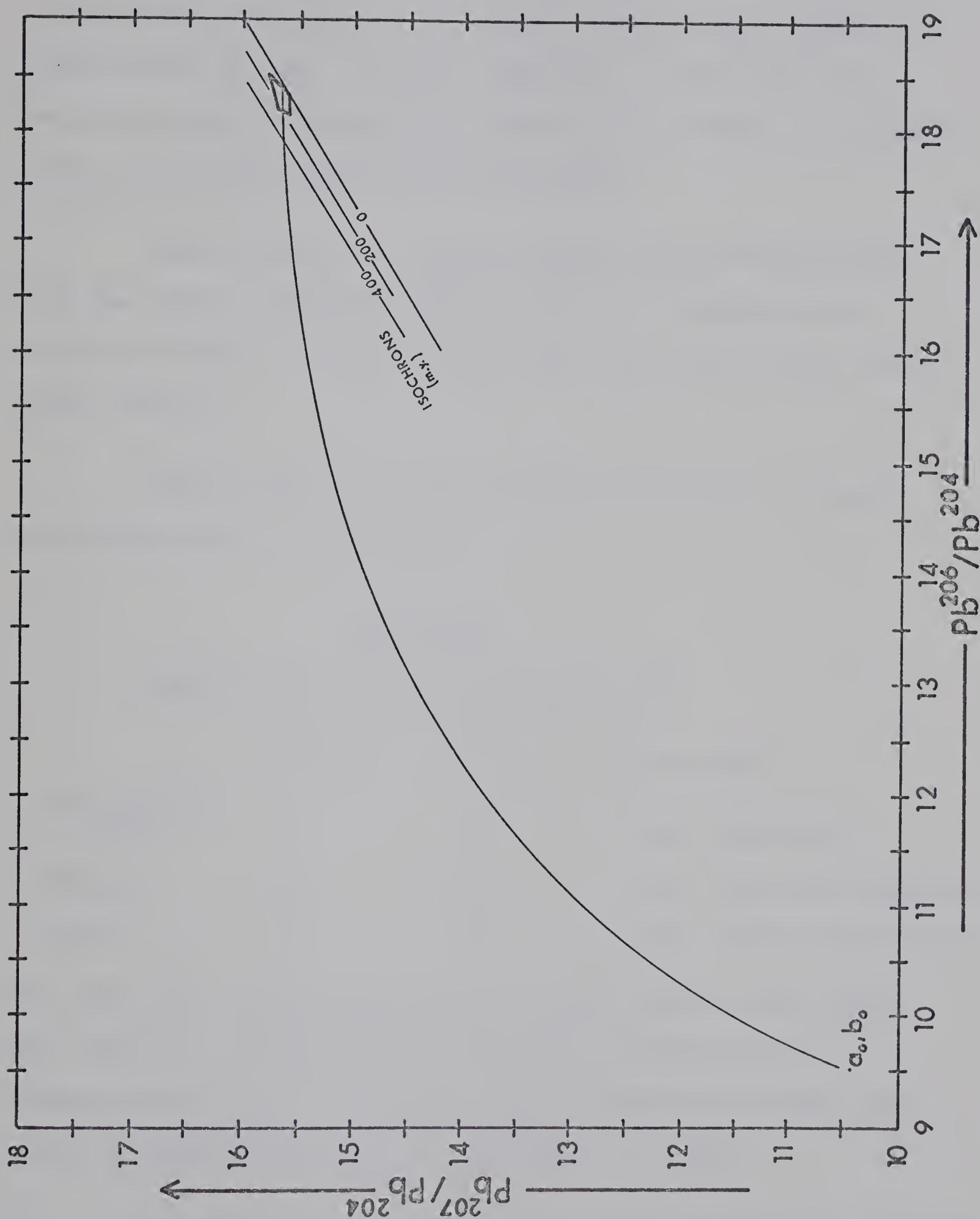


Fig. 4.5 Pb^{207}/Pb^{204} - Pb^{206}/Pb^{204} plot showing position of Irish leads with respect to primary growth curve of Cooper ($\mu=8.79$).

such acute angles, that a slight error in the measured ratio, when projected to the growth curve, would produce a large error in age. A small component of the error may be due to mass fractionation however this should not greatly affect the model ages determined below.

Model ages for a given ordinary lead should agree for the three lead-lead plots. Error in measurement of the Irish leads however is such that the ages do not agree very closely.

Model ages are given for the Silvermines, Tynagh and Ennis areas in Table 4.1.

Table 4.1

Single-Stage Model Age in yr. $\times 10^6$

	<u>y vs. x</u>	<u>z vs. x</u>	<u>z/x vs. y/x</u>
Silvermines Area	40	20	60 (Tertiary)
Tynagh	160	200	150 (Triassic-Jurassic)
Ennis	75	85	85 (Upper Cretaceous)

The ages for the deposits on the y vs. x plot range from 20 - 210 m.y. This range of 190 m.y., although not likely very exact, should be a good indication of the true range in model lead ages if the model is valid.

Inaccuracy in the dating of younger leads, in contrast to older leads, is obviously more significant. Accuracy of

the model age depends in part on accuracy of the measured ratios, but perhaps more on the accuracy of the geophysical constants used in calculating the growth curve. Techniques such as isotope spiking, multiple runs and interlaboratory standardization can produce results with a precision of better than 0.1%, but minor revisions in the geophysical constants can alter the model age interpretation very significantly. The geophysical constants have been revised several times in the past, and there is no reason to assume the most recent revision is the last. Although the model lead age may differ significantly from the true age, if the model assumptions are valid, the relative ages of the various deposits and the range in ages should be quite reliable because they are not very sensitive to a change in the geophysical constants used.

There is a very obvious geographic grouping of deposits with similar model ages as exemplified by the Silvermines, Tynagh and Ennis areas (Figure 4.1). There is also a regional geographic trend in model ages (Figures 4.2, 4.3 and 4.4) wherein the lead becomes progressively more radiogenic, or younger, from north to south, from Riofinex (oldest) through Tynagh and Ennis to Silvermines (youngest).

Four of the deposits studied (19, 20, 21, and 12) are veins which are located in Devonian sandstones or

Silurian shales. Lead ratios from these veins are isotopically similar to the geographically related Silvermines leads implying a common source and time of mineralization.

In summary, the absolute model age must be considered approximate, partly because of the error spread in the measurement of the lead ratios, and particularly because of the uncertainty in the accuracy of the geophysical constants used. Model ages can be most accurately determined on the y vs. x plot, which shows that model ages of Irish leads included in this study span a range of 190 m.y., from Lower Triassic to upper Tertiary. There is also a very definite grouping of model ages for geographically related samples, in other words, a definite isotopic fingerprinting.

Summary of Model Lead Interpretations

The Irish leads can be interpreted as single-stage or short period anomalous. Scatter in the data points is probably due largely to measurement error, as the scatter for geographically related samples is clearly linear and almost parallel to error lines. The measured ratios lie close to the single-stage growth curve ($\mu=8.79$) of Cooper et al. (1969). According to a single-stage interpretation, the lead was derived from a homogeneous system with respect to the ratios U:Th:Pb, which is characterized by the present

ratios $U^{238}/Pb^{204}=8.79$, $Th^{232}/Pb^{204}=36.4$ and $Th^{232}/U^{238}=4.14$.

Model ages (single-stage) span a range of 190 m.y. from Lower Triassic to upper Tertiary. Geographically related deposits have about the same model ages.

Age of Mineralization and Source of Metals - Other Evidence

Age of Mineralization

There are no conclusive geological criteria which significantly narrow the maximum-minimum range for the time of mineralization.

Most of the occurrences studied and the 4 major deposits occur in rocks of Lower Carboniferous, specifically Tournaisian - Viséan age, thereby setting a maximum age of 350 m.y. for the mineralization. An exception is the Gorteen Colliery vein which cuts Upper Carboniferous (Westphalian) coal measures somewhat greater than 270 m.y. in age.

After exhaustive study of sulphide deposits along the Silvermines Fault, Rhoden (1958) believed that the mineralization postdated the last major movements on the Fault. The last major movements were, he believed, almost certainly related to Hercynian (Permo-Carboniferous) orogenic disturbances. He therefore felt that mineralization was

post Hercynian or less than 270 m.y. Rhoden's studies however predate discovery of the Mogul orebody. The Mogul upper orebody differs in many important aspects from the lower orebody and other mineralization along the fault. A number of features of the upper orebody and the Magcobar barite deposit suggest that these deposits are syngenetic (Graham, 1970). It is conceivable that the Silvermines Fault was active during the Lower Carboniferous (there is some evidence of minor tectonic activity in the Lower Carboniferous) and acted as a channelway for ascending metaliferous solutions at that time. Mineralization could have continued throughout the Carboniferous and into the Permian, and other occurrences studied by Rhoden along the Silvermines Fault may in fact be much younger than the Mogul upper orebody.

The Tynagh, Gortdrum and Riofinex deposits are similarly controlled by faults on which major displacements probably took place in Hercynian times. These faults too, however, may have been active in Lower Carboniferous times.

A minimum Tertiary age (not more accurately dated) was determined for the Tynagh mineralization based on the dating of fragments of Sequoia and Cypress in the residual sulphide ore. Obviously this does not significantly narrow down the time of the Tynagh mineralization.

If the Mogul upper orebody is indeed syngenetic, then the model lead ages of 40 m.y. for the upper orebody and the Magcobar deposit are clearly not meaningful. Evidence for syngenetic formation of the upper orebody and the Magcobar deposit is however not unequivocal. It must be concluded that the model ages for leads included in this study, which range from 20-210 m.y., are not contradicted by any conclusive geological evidence.

Source of Metals

Temperatures of formation of the Mogul orebody and sulphur isotope ratios for sulphides from the Mogul, Tynagh and Gortdrum orebodies suggest a deep source region for the metals.

Temperatures of deposition for the Mogul mine based on filling temperatures of fluid inclusions and on sulphur isotope geothermometry (Greig et al., 1971) range from 150°C to 350°C and average about 250°C. Such high temperatures would suggest that the metaliferous solutions originated at considerable depth or alternatively circulated to considerable depth.

It is very unlikely that the hydrothermal solutions leached the metals from higher level post-Caledonian (Devonian to Cretaceous) lithologies and travelled directly

downward or laterally to the site of deposition. The aggregate thickness of sediments representing the period from Devonian to Cretaceous would not have exceeded 10,000 feet in any part of Ireland, and normal geothermal gradients would not be sufficiently high to account for the temperatures reached by the ore forming fluids. Furthermore there is no evidence for abnormal geothermal gradients consistently applicable to all localities of sulphide mineralization.

It is possible that the fluids originated in higher level post-Caledonian sediments, percolated to deep levels and leached the metals from Lower Paleozoic or deeper rocks and then ascended along favorable structural channelways (faults) ultimately depositing the metals in a comparatively near surface environment. It seems more plausible that the metaliferous fluids originated at depth in the Lower Paleozoic rocks as connate water. A third possibility is that the solutions were magmatically derived.

Russell (1968), who favoured a Lower Paleozoic source for the metals, analysed 63 samples of Ordovician and Silurian greywackes and shales, and showed that these sediments contain more than adequate quantities of lead-zinc-copper and barium. (20, 100, 45 and 700 ppm respectively) such that only extremely small percentages

of these metals originally contained in the sediments would be required to account for all of the known mineralization.

In summary, if the source was not magmatic, the solutions must have originated at, or at least circulated to considerable depth in order to have attained the temperatures indicated, a depth which far exceeded that of the maximum depth of burial of Upper Paleozoic or younger lithologies.

Sulphur isotope studies reveal a large spread in δS^{34} values (+4% to -33%) for sulphides from the Mogul, Tynagh and Gortdrum deposits. However, the δS^{34} values for samples taken close to the respective faults are near meteoritic ($\pm 5\%$). With increasing distance from the faults the δS^{34} ratios become progressively more negative. This pattern in the Mogul deposit is most easily explained as due to isotopic fractionation between sulphide and sulphate in response to increase in Eh and pH and decrease in temperature (Greig et al.). Accordingly the δS^{34} values for the hydrothermal fluids, on first reaching the site of deposition, were close to meteoritic. The source environment must therefore have been capable of producing solutions containing sulphur isotopically close to meteoritic composition.

Either the source rocks are homogeneous and contain sulphur isotopically close to meteoritic values, or the sulphur accessible to solution in the source rocks has a mean isotopic composition close to that of meteoritic sulphur and homogenization has taken place in the hydrothermal fluid itself. There is no obvious biogenic or marine sulphate isotopic component. It seems unlikely that shallow marine and non-marine sediments of the Upper Paleozoic and younger rocks could produce fluids containing sulphur isotopically close to meteoritic values. On the basis of the sulphur isotope evidence along then, there appear to be only two possible sources for the sulphur. It could be magmatically derived (crustal or mantle) or alternatively it could be derived from the Lower Paleozoic sedimentary-volcanic eugeosynclinal assemblage.

In summary, only two sources are in accord with both the temperature of the ore forming fluids and the sulphur isotope evidence; a mantle or crustal magmatic source and a Lower Paleozoic sedimentary source.

Validity of the Lead Model

Validity of the lead model interpretation depends on the validity of the assumptions of the model. Leads from numerous deposits throughout the world of widely differing ages, many of which can be distinguished on the

basis of geological criteria alone, plot on a single lead growth curve defined by particular $\mu(U^{238}/Pb^{204})$ and $W(Th^{232}/Pb^{204})$ ratios. In order to explain the conformity to a single growth curve, it is necessary to invoke some homogeneous source which has existed on a global scale since the time of formation of the earth. Since no possible upper crustal source was recognized which met the above prerequisite, the source of these leads was assumed to the lower crust or mantle.

Studies by Ulrych (1967), Tatsumoto (1966a and 1966b), Lovering and Tatsumoto (1968) and others, have cast some doubt on the basic assumptions that the mantle is homogeneous with respect to the ratios U/Pb, Th/Pb and Th/U. Shaw (1957), Cannon et al. (1961) and Richards (1971b) have suggested or hinted that marine sediments might be sources of apparently ordinary leads. This author independently arrived at the same conclusion (briefly outlined in Chapter II. A sedimentary source model accounts for the constancy of the μ and W ratios and the ratio W/μ characteristic of ordinary leads. Earlier suggestions of a possible sedimentary source encountered the difficulty of explaining the constancy in the μ , W and W/μ ratios.

Speculative Interpretation Based on Sedimentary Source Model

Some brief speculation on a possible sedimentary source of the Irish leads, and recommendations for investigations which may substantiate the source are warranted.

Possible marine sedimentary sources for the Irish leads which have the necessary distribution are limited to Ordovician and Silurian eugeosynclinal sediments, or to Lower Carboniferous shales and argillaceous carbonates. The Lower Carboniferous Culm shales are of limited geographic extent, being restricted to the southernmost part of Ireland, and are excluded as a possible source on this basis. All the Lower Carboniferous lithologies would appear to be excluded as a likely source on several accounts. Firstly, the volume of Lower Carboniferous shales, or shaly limestones, excluding the Culm, does not appear to be sufficient to account for the tonnages of the metals contained in the known deposits if the contained metals are in normal concentrations for shales. Secondly, as discussed in the previous section, temperatures of precipitation of sulphides are unlikely to have ever been attained at the maximum depth of burial of the Carboniferous. Thirdly, it is unlikely that the mean δS^{34} ratio for sulphur in Lower Carboniferous shales would be close to the meteoritic

value of 0‰, considering the shallow marine depositional environment and the expected weighting of the sulphur isotopes toward either sea water sulphate or biogenic sulphur.

Ordovician and Silurian eugeosynclinal sedimentary rocks have been downfolded to great depths where temperatures of 250°C are likely, and the assemblage contains a large proportion of volcanic material which probably contains unfractionated sulphur isotopically close to 0‰. It has also been demonstrated by Russell (1968) that the Lower Paleozoics contain more than sufficient amounts of Pb, Zn, Cu and Ba.

The apparent range in model lead ages may result from episodic removal of lead from the sedimentary source rocks over a considerable time range, or alternatively the lead ores may all have been mineralized in a single episode. Leads isolated after a long residence time in the sediment would be enriched by the addition of radiogenic lead produced by the decay of U and Th in the sediment. In contrast, leads isolated soon after deposition of the sediment would not be significantly changed by the addition of new radiogenic lead and would reflect the isotopic composition of the lead in the sediment at the time it was deposited. If the lead ores were mineralized at different times, and if mixing were incom-

plete, the data would define a series of anomalous lead lines. If all the lead ores were mineralized in a single episode, the data would define a single anomalous lead line. Bearing in mind the maximum possible duration of the residence time in the sediment, Lower Paleozoic to the present, the leads would be short period anomalous leads.

Further work to test the validity of a proposed sedimentary source would require very accurate determination of isotope ratios for lead in the sulphide deposits and in the possible sedimentary source rocks. It should be possible with very precise data to recognize an anomalous lead line which, as discussed above, reflects the addition of radiogenic lead produced during the residence time in the sediment. It would be possible then to project this anomalous line back to the single-stage growth curve thereby enabling one to calculate the residence time in the sediment. Knowing the age of the sediment would then make it possible to determine the time of mineralization.

BIBLIOGRAPHY

- Alpher, R.A., and Herman, R.C., 1951, The primeval lead isotope abundances and the age of the earth's crust; *Phys. Rev.*, vol. 84, p. 1111-1114.
- Ashby, D.F., 1939, The geological succession and petrology of the Lower Carboniferous volcanic area of County Limerick; *Geol. Assoc. Proc.*, vol. 50, p. 324-330.
- Austin, C.F., and Slawson, W.F., 1961, Isotopic analyses of single galena crystals: a clue to the history of deposition; *Amer. Miner.*, vol. 46, p. 1132-1140.
- Bishopp, D.W., 1943, A short review of Irish mineral resources; *Geol. Surv. Ireland, Emergency Period Pamphlet no. 1*.
- Black, W.W., 1952, The origin of the supposed tufa bands in Carboniferous reef limestone; *Geol. Mag.*, vol. 80, p. 195-200.
- Brown, J.S., 1962, Ore leads and isotopes; *Econ. Geol.*, vol. 57, p. 673-720.
- Brown, J.S., 1965, Oceanic lead isotopes and ore genesis; *Econ. Geol.*, vol. 60, p. 47-68.
- Bullerwell, W., 1961, The gravity map of Northern Ireland; *Irish Naturalist Jour.*, vol. 13, p. 255-257.
- Cahen, L., Eberhardt, P., Geiss, J., Houtermans, F.G., Jedwab, J., and Signer, P., 1958, On a correlation between the common lead model age and the trace-element content of galenas; *Geochim. et Cosmochim. Acta*, vol. 14, p. 134-149.

- Cannon, Jr., R.S., Pierce, A.P., Antweiler, J.C., and Buck, K.L., 1961, The data of lead isotope geology related to problems of ore genesis; *Econ. Geol.*, vol. 56, p. 1-38.
- Catanzaro, E.J., and Gast, P.W., 1960, Isotopic composition of lead in pegmatitic feldspars; *Geochim. et Cosmochim. Acta*, vol. 19, p. 113-126.
- Catanzaro, E.J., 1968, Absolute isotopic abundance ratios of three common lead reference samples; *Earth and Planet. Sci. Letters*, vol. 3, p. 343-346.
- Charlesworth, J.K., 1963, *Historical geology of Ireland*; Oliver and Boyd, Edinburgh, 565 p.
- Chow, T.J., and Patterson, C.C., 1959, Lead isotopes in manganese nodules; *Geochim. et Cosmochim. Acta*, vol. 17, p. 21-31.
- Chow, T.J., and Patterson, C.C., 1962, The occurrence and significance of lead isotopes in pelagic sediments; *Geochim. et Cosmochim. Acta*, vol. 26, p. 263-308.
- Chow, T.J., and Johnstone, 1964, Lead isotopes in sediments of three Canadian Shield lakes (Abstract); *Trans. Amer. Geophys. Union*, vol. 45, p. 110-111.
- Cole, G.A.J., 1922, Memoir and map of localities and minerals of economic importance and metalliferous mines in Ireland; *Mem. Geol. Surv. of Ireland*, Dublin, 1922 (reprinted 1956), 155 p.
- Cooper, J.A., Richards, J.R., 1966, Lead isotopes and volcanic magmas; *Earth and Planet. Sci. Letters*, vol. 1, p. 259-269.
- Cooper, J.A., Reynolds, P.H., Richards, J.R., 1969, Double-spike calibration of the Broken Hill standard lead; *Earth and Planet. Sci. Letters*, vol. 6, p. 467-470.

- Collins, C.B., Russell, R.D., and Farquhar, R.M., 1953, The maximum age of the elements and the age of the earth's crust; Can. Jour. of Phys., vol. 31, p. 402-418.
- Damon, P.E., 1954, An abundance model for lead isotopes based upon the continuous creation of the earth's sialic crust; Trans. Amer. Geophys. Union, vol. 35, p. 631-635.
- Delepine, G.G., 1951, Studies of the Devonian and Carboniferous of western Europe and north Africa; Proc. Geol. Assoc. Lond., vol. 62, p. 140-166.
- Derry, D.R., Clark, G.C., and Gillat, N., 1965, The Northgate base metal deposit at Tynagh, County Galway, Ireland; Econ. Geol., vol. 60, p. 1218-1237.
- Doe, E.R., 1962, Relationships of lead isotopes among granites, pegmatites and sulfide ores near Balmat, New York; Jour. Geophys. Res., vol. 67, p. 2895-2906.
- Doe, B.R., Tilton, G.R., and Hopson, C.A., 1965, Lead isotopes in feldspars from selected granitic rocks associated with regional metamorphism; Jour. Geophys. Res., vol. 70, p. 1947-1968.
- Doe, B.R., Hedge, C.E., White, D.E., 1966, Preliminary investigation of the source of lead and strontium in deep geothermal brines underlying the Salton Sea geothermal area; Econ. Geol., vol. 61, p. 462-483.
- Douglas, J.A., 1909, The Carboniferous limestone of County Clare; Geol. Soc. Lond. Quart. Jour., vol. 65, p. 538-586.
- Eberhardt, P., Geiss, J., and Houtermans, F.G., 1955, Isotopic ratios of ordinary leads and their significance; Z. Phys., vol. 134, p. 91-102.

- Farquhar, R.M., and Cumming, G.L., 1954, Isotopic analyses of anomalous lead ores; Royal Soc. of Can. Trans., vol. 48, p. 9.
- Farquhar, R.M., and Russell, R.D., 1957, Anomalous leads from the Upper Great Lakes region of Ontario; Trans. Amer. Geophys. Union, vol. 38, p. 552-556.
- Farquhar, R.M., and Russell, R.D., 1963, A monograph for the interpretation of anomalous lead isotope abundances; Geochim. et Cosmochim. Acta, vol. 27, p. 1143-1148.
- Finlayson, 1910, The metallogeny of the British Isles; Quart. Jour. Geol. Soc. Lond., vol. 66, p. 281-296.
- George, T.N., 1958, Lower Carboniferous paleogeography of the British Isles; Yorkshire Geol. Soc. Proc., vol. 31, p. 277-318.
- Gill, W.D., 1962, Some aspects of the Variscan fold belt; Manchester Press, ed. Coe, B.K., Chapt. 3.
- Graham, J.A., 1970, Unpublished Ph.D. thesis, University of Western Ontario.
- Green, D.H., 1968, Unpublished Ph.D. thesis, University of Alberta.
- Greig, J.A., Baadsgaard, H., Cumming, G.L., Folinsbee, R.E., Krouse, H.R., Ohmoto, H., Sasaki, A., Smeykal, V., 1971, Lead and sulphur isotopes of the Irish base metal mines in Carboniferous carbonate host rocks; Proc. IMA-IAGOD meetings '70, Joint Symp., vol., p. 84-92.
- Hamilton, E.I., 1966, The isotopic composition of lead in igneous rocks; Earth and Planet. Sci. Letters, vol. 1, p. 30-37.

- Hamilton, E.I., and Farquhar, R.M., 1968, Radiometric Dating for Geologists; Interscience Publishers, New York, 506 p.
- Heier, K.S., and Rogers, J.J.W., 1963, Radiometric determination of thorium, uranium and potassium in basalts and in two magmatic differentiation series; *Geochim. et Cosmochim. Acta*, vol. 27, p. 137-154.
- Heier, K.S., and Adams, J.A.S., 1965, Concentration of radioactive elements in deep crustal material; *Geochim. et Cosmochim. Acta*, vol. 29, p. 53-61.
- Heyl, A.V., Delevaux, M.H., Zartman, R.E., and Brock, M.R., 1966, Isotopic study of galenas from the upper Mississippi valley, the Illinois-Kentucky, and some Appalachian valley mineral districts; *Econ. Geol.*, vol. 61, p. 933-961.
- Hodson, F., 1954, The beds above the Carboniferous limestone in north-west County Clare, Eire; *Geol. Soc. Lond. Quart. Jour.*, vol. 109, p. 259-283.
- Hodson, F., and Lewarne, G.C., 1961, A mid-Carboniferous (Namurian) basin in parts of the counties of Limerick and Clare, Ireland; *Geol. Soc. Lond. Quart. Jour.*, vol. 117, p. 307-333.
- Holmes, A., 1946, An estimate of the age of the earth; *Nature*, vol. 157, p. 680-684.
- Holmes, A., 1947, A revised estimate of the age of the earth; *Nature*, vol. 159, p. 127-128.
- Holmes, A., 1949, Lead isotopes and the age of the earth; *Nature*, vol. 163, p. 453-456.
- Houtermans, F.G., 1946, The isotope ratios in natural lead and the age of uranium; *Naturwissenschaften*, vol. 33, p. 185-186.

- Jeffreys, H., 1948, Lead isotopes and the age of the earth; *Nature*, vol. 162, p. 822-823.
- Jeffreys, H., 1949, Lead isotopes and the age of the earth; *Nature*, vol. 164, p. 1046.
- Kanasewich, E.R., 1962a, Approximate age of tectonic activity using anomalous lead isotopes; *Royal Astron. Soc. Geophys. Jour.*, vol. 7, p. 158-168.
- Kanasewich, E.R., 1962b, Quantitative interpretations of anomalous lead isotope abundances; Unpublished Ph.D. Thesis, University of British Columbia.
- Kanasewich, E.R., and Slawson, W.F., 1964, Precision intercomparisons of lead isotope ratios, Ivigtut, Greenland; *Geochim. et Cosmochim. Acta*, vol. 28, p. 541-549.
- Kollar, F., Russel, R.D., and Ulyrch, T.J., 1960, Precision intercomparisons of lead isotope ratios, Broken Hill and Mount Isa; *Nature*, vol. 187, p. 754-756.
- Kollar, F., 1960, The precise intercomparison of lead isotope ratios; Unpublished Ph.D. thesis, Department of Physics, University of British Columbia, Canada.
- Leech, G.B., and Wanless, R.K., 1962, Lead isotope and potassium-argon studies in the East Kootenay district of British Columbia; *Geol. Soc. Amer., Buddington Vol.*, p. 241-280.
- Lees, A., 1961, The Waulsortian Reefs of Eire; a carbonate mud bank complex of Lower Carboniferous age; *Jour. Geol.*, vol. 69, p. 101-109.
- Lees, A., 1964, The structure and origin of the Waulsortian (Lower Carboniferous) Reefs of west-central Eire; *Phil. Trans. Royal Soc. Lond., Series B*, no. 740, vol. 247, p. 483-531.

- Long, A., Silverman, A.J., and Kulp, J.L. 1960, Isotopic composition of lead and Pre-cambrian mineralization of the Coeur D'Alene district, Idaho; Econ. Geol., vol. 55, p. 645-658.
- Lovering, J.F., and Tatsumoto, M., 1968, Lead isotopes and the origin of granulite and eclogite inclusions in deep-seated pipes; Earth and Planet. Sci. Letters, vol. 4, p. 350-356.
- Moorbath, S., 1959, Isotopic composition of lead from British mineral deposits; Nature, vol. 183, p. 595-596.
- Moorbath, S., 1962, Lead isotope abundance determination study on mineral occurrences in the British Isles etc; Phil. Trans. Royal Soc., Series A, vol. 254, p. 295-360.
- Murthy, V.R., and Patterson, C.C., 1961, Lead isotopes in ores and rocks of Butte, Montana; Econ. Geol., vol. 56, p. 59-67.
- Murthy, V.R., and Patterson, C.C., 1962, Primary isochron of zero age for meteorites and the earth; Jour. Geophys. Res., vol. 67, p. 1161-1167.
- Nevill, W.E., 1958, The Carboniferous knoll-reefs of east central Ireland; Royal Irish Acad. Proc., vol. 59, sec. B, no. 14, p. 285-303.
- Nier, A.O., 1938, Variations in the relative abundances of the isotopes of common lead from various sources; Jour. Amer. Chem. Soc., vol. 60, p. 1571-1576.
- Nier, A.O., Thompson, R.W., and Murphey, B.F., 1941, The isotopic constitution of lead and the measurement of geologic time, III; Phys. Rev., vol. 60, p. 112.
- O'Brien, M.V., 1958a, The mineral deposits of the Republic of Ireland; Inst. Min. Metall. Symposium, no. 1.

- O'Brien, M.V., 1958b, Economic geology of Ireland; Adv. Sci., no. 56, p. 349-352.
- Ostic, R.G., 1962, Isotopic composition of eastern Australian leads; Jour. Geophys. Res., vol. 67, p. 1651-1652.
- Ostic, R.G., Russell, R.D., and Reynolds, P.H., 1963, A new calculation for the age of the earth from abundances of lead isotopes; Nature, vol. 199, p. 1150-1152.
- Ostic, R.G., Russell, R.D., and Stanton, R.L., 1967, Additional measurements of the isotopic composition of lead from stratiform deposits; Can. Jour. Earth Sci., vol. 4, p. 245-269.
- Oversby, V.M., 1970, The isotopic composition of lead in iron meteorites; Geochim. et Cosmochim. Acta, vol. 34, p. 65-75.
- Oversby, V.M., and Gast, P.W., 1970, Isotopic composition of lead from oceanic islands; Jour. Geophys. Res., vol. 75, p. 2097-2114.
- Parkinson, D., 1957, Lower Carboniferous reefs of northern England; Bull. Amer. Assoc. Pet. Geol., vol. 41, p. 511-537.
- Patterson, C.C., 1953, The isotopic composition of meteoritic, basaltic, and oceanic leads and the age of the earth; Proc. First Conf. on Nuclear Processes in Geological Settings, p. 36-40.
- Patterson, C.C., 1955, The $\text{Pb}^{207}/\text{Pb}^{206}$ ages of some stone meteorites; Geochim. et Cosmochim. Acta, vol. 7, p. 151-153.
- Patterson, C.C., Tilton, G., and Inghram, M.G., 1955, Age of the earth; Science, vol. 121, p. 69-75.

- Patterson, C.C., 1956, Age of meteorites and the earth; *Geochim. et Cosmochim. Acta*, vol. 10, p. 230-237.
- Patterson, C.C., and Duffield, B., 1963, The isotopic composition of lead in Easter Island rhyolite; *Geochim. et Cosmochim. Acta*, vol. 27, p. 1180-1181.
- Patterson, C.C., 1964, Characteristics of lead isotope evolution on a continental scale in the earth; *Isotopic and Cosmic Chemistry*, Chapt. 19, North-Holland Publishing Company, Amsterdam, p. 244-268.
- Pockley, R.P.C., 1961, Lead isotope and age studies of uranium and lead minerals from the British Isles and France; Unpublished Ph.D. thesis, University of Oxford.
- Rhoden, H.N., 1958, Structure and economic mineralization of the Silvermines district, County Tipperary, Eire; *Trans. Inst. Min. Metall.*, vol. 68, p. 67-94.
- Richards, J.R., 1962, Isotopic composition of Australian leads; *Jour. Geophys. Res.*, vol. 67, p. 869-884.
- Richards, J.R., 1963, Isotopic composition of Australian leads - III: Northwestern Queensland and the Northern Territory - A reconnaissance; *Geochim. et Cosmochim. Acta*, vol. 27, p. 217-240.
- Richards, J.R., 1968, "Primary" leads; *Nature*, vol. 219, p. 258-259.
- Richards, J.R., 1971a, Major lead orebodies - mantle origin?; *Econ. Geol.*, vol. 66, p. 425-434.
- Richards, J.R., 1971b, The evidence from lead isotopes on the immediate source of lead in ore forming solutions; *Contrib. to Internat. Geochim. Cong. Moscow*, July.

- Russell, M.J., 1968, Structural controls of base metal mineralization in Ireland in relation to continental drift; Trans. Instn. Min. Metall., vol. 77, p. B117-B128.
- Russell, R.D., Farquhar, R.M., Cumming, G.L., and Wilson, J.T., 1954, Dating galenas by means of their isotopic constitutions; Trans. Amer. Geophys. Union, vol. 35, p. 301-309.
- Russell, R.D., and Allan, D.W., 1956, The age of the earth from lead isotope abundances; Royal Astron. Soc. Monthly Notices, Geophys. Suppl. 7, p. 80-101.
- Russell, R.D., 1956, Interpretations of lead isotope abundances; Proc. 2nd Conf. on Nuclear Processes in Geol. Settings, p. 68-78.
- Russell, R.D., and Farquhar, R.M., 1960a, Lead isotopes in geology; Interscience Publishers, Inc., New York, 243 p.
- Russell, R.D., and Farquhar, R.M., 1960b, Dating galenas by means of their isotopic constitutions - II; Geochim. et Cosmochim. Acta, vol. 19, p. 41-52.
- Russell, R.D., Ulrych, T.J., and Kollar, F., 1961, Anomalous leads from Broken Hill, Australia; Jour. Geophys. Res., vol. 66, p. 1495-1498.
- Russell, R.D., 1963, Some recent researches on lead isotope abundances; Earth Sci. and Meteorites, North-Holland Publishing Co., Amsterdam, p. 44-73.
- Russell, R.D., Slawson, W.F., Ulrych, T.J. and Reynolds, P.H., 1967, Further applications of concordia plots to rock lead isotope abundances; Earth and Planet. Sci. Letters, vol. 3, p. 284-288.
- Schultz, R.W., 1966, Lower Carboniferous cherty ironstones at Tynagh, Ireland; Econ. Geol., vol. 61, p. 311-342.

- Schwarzacher, W., 1961, Petrology and structure of some Lower Carboniferous reefs in northeastern Ireland; Bull. Amer. Assoc. Pet. Geol., vol. 45, p. 1481-1503.
- Shaw, D.M., 1957, Comments on the geochemical implications of lead isotope dating of galena deposits; Econ. Geol., vol. 52, p. 570-573.
- Shepard-Thorn, E.R., 1963, The Carboniferous limestone succession in north-west County Limerick, Ireland; Proc. Royal Irish Acad., sec. B, no. 62, p. 267-294.
- Sinclair, A.J., 1965, Volume of source rocks of the radiogenic component of (anomalous) lead deposits; Econ. Geol., vol. 60, p. 1709-1717.
- Sinclair, A.J., 1966, Anomalous leads from the Kootenay area British Columbia; Can. Inst. Min. and Metall., Special vol. 8, p. 249-262.
- Slawson, W.F., and Austin, C.F., 1962, A lead isotope study defines a geological structure; Econ. Geol., vol. 57, p. 21-29.
- Smyth, L.B., 1939, The Lower Carboniferous of south-east Ireland; Geol. Assoc. Proc., vol. 50, p. 305-319.
- Snelgrove, A.K., 1966a, Irish "strata bound" base metal deposits (Part 1); Can. Min. Jour., vol. 47, p. 47-53.
- Snelgrove, A.K., 1966b, Irish "strata bound" base metal deposits (Part 2); Can. Min. Jour., vol. 47, p. 55-60.
- Stanton, R.L., 1955, The genetic relationship between limestone, volcanic rocks and certain ore deposits; Austral. Jour. Sci., vol. 17, p. 173.
- Stanton, R.L., and Russell, R.D., 1959, Anomalous leads and the emplacement of lead sulphide ores; Econ. Geol., vol. 54, p. 588-607.

- Stanton, R.L., and Rafter, T.A., 1966, The isotopic constitution of sulphur in some strataform lead zinc sulphide ores; *Mineralium Deposita*, vol. 1, p. 16-29.
- Tatsumoto, M., 1966a, Isotopic composition of lead in volcanic rocks from Hawaii, Iwo Jima, and Japan; *Jour. Geophys. Res.*, vol. 71, no. 6, p. 1721-1733.
- Tatsumoto, M., 1966b, Genetic relations of oceanic basalts as indicated by lead isotopes; *Science*, vol. 153, p. 1094-1101.
- Thompson, I.S., 1967, The discovery of the Gortdrum deposit, County Tipperary, Ireland; *Can. Inst. Min. and Metall.*, vol. 70, p. 85-92.
- Tilton, G.R., Patterson, C.C., Brown, H., Inghram, M., Hayden, R., Hess, D., and Larsen, E., 1955, Isotopic composition and distribution of lead uranium and thorium in a Precambrian granite; *Bull. Geol. Soc. Amer.*, vol. 66, p. 1113-1148.
- Tilton, G.R., 1956, The interpretation of lead age discrepancies by acid washing experiments; *Trans. Amer. Geophys. Union*, vol. 37, p. 224-230.
- Tilton, G.R., and Reed, G.W., 1960, Concentration of lead in ultramafic rocks by neutron activation analysis; (Abstract), *Jour. Geophys. Res.*, vol. 65, p. 2529.
- Tilton, G.R., 1960, Volume diffusion as a mechanism for discordant lead ages; *Jour. Geophys. Res.*, vol. 65, p. 2933-2945.
- Tilton, G.R., and Steiger, R.H., 1965, Lead isotopes and the age of the earth; *Science*, vol. 150, p. 1805-1807.
- Turekian, K.K., and Wedepohl, K.H., 1961, Distribution of the elements in major units of the earth's crust; *Geol. Soc. Amer. Bull.*, vol. 72, p. 175-192.

- Turner, J.S., 1952, The Lower Carboniferous rocks of Ireland; Liverpool and Manchester Geol. Jour., vol. 1, p. 113-147.
- Ulrych, T.J., and Russell, R.D., 1964, Gas source mass spectrometry of trace leads from Sudbury, Ontario; Geochim. et Cosmochim. Acta, vol. 28, p. 455-469.
- Ulrych, T.J., 1964, The anomalous nature of Ivigtut lead; Geochim. et Cosmochim. Acta, vol. 28, p. 1389-1396.
- Ulrych, T.J., 1967, Oceanic basalt leads: a new interpretation and an independent age for the earth; Science, vol. 158, p. 252-256.
- Vaasjoki, O., and Kouvo, O., 1959, A comparison between the common lead isotopic composition and minor base metal contents of some Finnish galenas; Econ. Geol., vol. 54, p. 301-307.
- Welke, H., Moorbath, S., Cumming, G.L., and Sigurdsson, H., 1968, Lead isotope studies on igneous rocks from Iceland; Earth and Planet. Sci. Letters, vol. 4, p. 221-231.
- Wilson, J.T., Russell, R.D., and Farquhar, R.M., 1956, Radioactivity and age of minerals; Handbuch der Physik., vol. 47, p. 288-363.

APPENDIX I

Mineralogy, Host Rocks and Structural Control of Minor Base Metal Occurrences

Name of Deposit	Map No.	Structural Control	Host Rocks*	Mineralogy**	Location
Rinville	2	Irregular fracture fillings and re- placement	Upper Carb. Limestone	gn - sph - py	52° 15' 5" N 8° 58' 55" W
Tynagh (Carhoon)	4	Veinlets in dolo- mite about 250' above base of Carb.-2 miles south of Tynagh Fault.	Lower Carb. Limestone - lower dolo- mite	gn	53° 9' 40" N 8° 21' 5" W
Caherglasaun	5	No definite vein - confined to irregular calcite body.	Upper Carb. Limestone	gn - tet - bour - cal	53° 6' 10" N 8° 53' 15" W
Milltown	6	Replacement in lime- stone about 1000' above base of Carb.	Lower or Middle Carb. Limestone	ccp - sph - gn - cal	52° 52' 5" N 8° 47' 30" W
Ballyvergin	7	?	Lower Lime- stone Shale	ccp - gn - sph - asp - cal	52° 52' 50" N 8° 51' 40" W
Crowhill	8	Replacement in lime- stone	Lower Carb. Limestone	gn - sph - ccp - py - cobalt minerals - cal	52° 51' 55" N 8° 50' 20" W

Name of Deposit	Map No.	Structural Control	Host Rocks*	Mineralogy**	Location
Monanoe	9	Replacement in limestone about 1,000' above base of Carb.	Lower Carb. Limestone	ccp - gn - asp - cal	52° 50' 35" N 8° 53' 35" W
Ballyhickey	10	Replacement in dolomite	Lower Carb. Limestone - magnesian dolomite	gn - sph - ccp - asp - cal	52° 50' 20" N 8° 51' 50" W
Kilbreckan	11	Replacement in limestone about 1,000' above base of Carb.	Middle or Lower Carb. Limestone	gn - sph - asp	52° 50' 25" N 8° 53' 35" W
Garrane	12	Brecciated veins.	Silurian grits and siltstones	gn - ccp - py - qtz - cal	52° 50' 10" N 8° 3' 5" W
Magcobar Barite Mine	14	Stratiform replacement (?) of lower dolomite near Silvermines Fault.	Lower Carb. Limestone - lower dolomite	bar - py - gn - sph	52° 47' 30" N 8° 15' 10" W
Gorteenadiha	15	On Silvermines Fault.	Lower Limestone Shales	gn - py - ccp - qtz	52° 47' 30" N 8° 16' 40" W
Ballynoe	16	On Silvermines Fault.	Lower Carb. limestone - lower dolomite	gn - py - ccp - sph - qtz	52° 47' 5" N 8° 15' 20" W

Name of Deposit	Map No.	Structural Control	Host Rocks*	Mineralogy**	Location
Knockanroe	17	On Silvermines Fault	Lower Carb. Limestone - lower dolomite	gn - py - ccp - sph - qtz	52° 47' 10" N 8° 14' 30" W
Shallee	18	Vein in brecciated rock close to Sil- vermines Fault and at the base of the Carb.	Devonian sand- stones and Lower Lime- stone Shales	gn - qtz - cal	52° 47' 15" N 8° 17' 15" W
Name Unknown	19	Veins occupying fractures related to Silvermines Fault	Devonian sandstones	gn - bar - qtz	52° 47' 0" N 8° 17' 30" W
Gortshanroe	20	Fracture filling and replacement	Silurian siltstone	sph - gn - bar - sid - qtz	52° 47' N 8° 15' W
Kileen	21	Vein	Silurian shales and Devonian sandstones	ccp - gn - py - sph - tet - bar - sid	52° 44' 45" N 8° 19' 00" W
Cloghatrida	22	Veins striking E-W dipping 70° N	Lower Carb. Limestone - dolomite	gn - sph - ccp - cal	52° 32' 25" N 8° 57' 50" W

Name of Deposit	Map No.	Structural Control	Host Rocks*	Mineralogy**	Location
Gorteen Colliery	24	Small fracture filling	Coal Measures gn - cal (Upper Carboni- ferous)		Slieve Ardah Coalfield TIP 49/3

*Geological Survey of Eire lithostratigraphic subdivisions of Carboniferous are capitalized. General host rock type is not capitalized.

**Mineral abbreviations:

asp = arsenopyrite	py = pyrite
bar = barite	qtz = quartz
bour = bournonite	sid = siderite
cal = calcite	sph = sphalerite
ccp = chalcopyrite	tet = tetrahedrite
gn = galena	

APPENDIX II

Preparation of Reagents and Extraction Procedures

Preparation of Reagents

- Chloroform: Use stock CHCl_3 - Wash with 50 ml. 3N HCl several times in large separation funnel - Wash once with 3 x distilled lead free water.
- Dithizone: Dissolve 10 mg. diphenylthiocarbazone in 100 ml. purified CHCl_3 - Wash 3 x with 1 ml. 0.5% HCl and with 20 ml. distilled water (1 ml. = 40 ug Pb).
- Citrate: Dissolve 300 gm. dibasic NH_4 citrate in 500 ml. 3 x distilled water - Boil to drive off CO_2 - Bubble through NH_3 to pH 8.5-9 - Filter - Wash 1 x with 25 ml. dithizone and 5 x with CHCl_3 - Make up to 1 liter (30% solution).
- KCN: Dissolve 2 gm. pure KCN in 100 ml. 3 x distilled water.
- Conc. NH_4OH : Bubble NH_3 through 3 x distilled water in polyethylene flask until volume increases by 50%.

HCl and HNO_3 : Prepared by redistilling from SiO_2 still.

Extraction Procedures

1. Digest tiny cube microscopically pure galena in 1:1 HNO_3 - Evaporate to dryness - Dissolve residue in 2 ml. 2% HNO_3 .
2. Add 20 ml. NH_4 citrate to lead solution in separation funnel - Adjust to pH 7-8 if necessary with HNO_3 or conc. NH_4OH .
3. Extract with 5 ml. 0.1% dithizone (200 mg. of Pb as Pb dithizonate) - Drain Pb dithizonate into 50 ml. beaker - Discard aqueous phase - Rinse funnel with 3 x D water (3 x distilled and demineralized) - Pour Pb dithizonate back into funnel.
4. Strip Pb from Pb dithizonate with 5-10 ml. HNO_3 - Discard dithizone - Rinse aqueous phase once with CHCl_3 to remove emulsified dithizone - Adjust to pH 8-9 with NH_4OH .
5. Add 10-12 ml. 2% KCN to aqueous phase in funnel.
6. Extract again with 4 ml. 0.1% dithizone - Drain Pb dithizonate into 50 ml. beaker through small kleenex plug to remove traces of aqueous phase - Discard aqueous phase - Rinse funnel well with 3 x D water - Pour Pb dithizonate back into funnel.
7. Strip Pb dithizonate with 2 ml. 2% HNO_3 - Discard

dithizone phase - Rinse once with CHCl_3 to remove emulsified dithizone - Pour aqueous phase out top of funnel (to avoid carrying through CHCl_3) into centrifuge tube (volume 3 ml.)

8. Adjust pH 4-5 with NH_4OH or HNO_3 if necessary (add drop by drop with stirring rod) - Seal centrifuge tube with parafilm - Heat in beaker of hot water.
9. Uncap centrifuge tube - Bubble through H_2S using Pasteur tube to precipitate Pb as fine PbS - Centrifuge to sediment fine PbS - Sample is ready for loading on mass. spec. filament - Run sample within few days or pH changes and Pb redissolves - Samples can be stored for longer periods by stopping procedure after stage 7.

B30012